

AD-A229 143 REPORT DOCUMENTATION PAGE

DTIC FILE COPY (2)

1a SECURITY CLASSIFICATION AUTHORITY SECRET		1b RESTRICTIVE MARKINGS	
2b DECLASSIFICATION/DOWNGRADING SCHEDULE NOV 19 1990		3 DISTRIBUTION/AVAILABILITY OF REPORT Approved for public release; distribution unlimited.	
4 PERFORMING ORGANIZATION REPORT NUMBER(S)		5 MONITORING ORGANIZATION REPORT NUMBER(S) AFOSR-TR-90 1151	
6a NAME OF PERFORMING ORGANIZATION Northwestern University	6b OFFICE SYMBOL (If applicable)	7a NAME OF MONITORING ORGANIZATION Air Force Office of Scientific Research/NE	
6c ADDRESS (City, State, and ZIP Code) Dept. of Materials Science and Engineering Evanston, IL 60208-3108		7b ADDRESS (City, State, and ZIP Code) Building 410 Bolling AFB, DC 20332-6448	
8a NAME OF FUNDING SPONSORING ORGANIZATION AFOSR	8b OFFICE SYMBOL (If applicable) NE	9 PROCUREMENT INSTRUMENT IDENTIFICATION NUMBER AFOSR-89-0043	
8c ADDRESS (City, State, and ZIP Code) Building 410 Bolling AFB, DC 20332-6448		10 SOURCE OF FUNDING NUMBERS	
		PROGRAM ELEMENT NO 61102F	TASK NO 2306
		WORK UNIT ACCESSION NO A1	WORK UNIT ACCESSION NO -
11 TITLE (Include Security Classification) Tailored Interfaces for Metal-Matrix Composites-Fundamental Considerations			
12 PERSONAL AUTHOR(S) Morris E. Fine and Julia R. Weertman			
13a TYPE OF REPORT Annual Technical	13b TIME COVERED FROM 10/1/89 TO 9/30/90	14 DATE OF REPORT (Year, Month, Day) October 31, 1990	15 PAGE COUNT
16 SUPPLEMENTARY NOTATION			
17 COSATI CODES		18 SUBJECT TERMS (Continue on reverse if necessary and identify by block number)	
FIELD	GROUP	SUB-GROUP	
		Metal matrix composites, interfaces, aluminum matrix, magnesium matrix, titanium carbide, silicon carbide, spinel	
19 ABSTRACT (Continue on reverse if necessary and identify by block number) The objective of this research is to determine the interface properties needed for successful metal matrix composites and to learn how to achieve these properties. A number of factors have been selected for study. These are thermodynamic stability of the interface, nature of the bonding across the interface, energy and structure of the interface, and role of adsorption at the interface. A number of systems have been chosen to probe these factors; namely, Al/TiC, Al/ α -Al ₂ O ₃ , Al/MgAl ₂ O ₄ (spinel), Al/Al ₃ (Ti _x , Zr _{1-x}), Mg/SiC, Mg/MgO, and Mg/Al ₂ O ₃ . Techniques for preparing all of these composites have been worked out, including mechanical alloying followed by extrusion, arc melting, and liquid metal infiltration. MMCs also were obtained from Martin Marietta and Dow. Microstructures of the resulting MMCs are presented and discussed along with preliminary studies of some of the interfaces using transmission electron microscopy. In comparison to Al/SiC, Al/TiC and Mg/SiC show no evidence of chemical reaction at the interface during processing. Al/MgAl ₂ O ₄ (spinel) has superior mechanical properties to Al/ α -Al ₂ O ₃ , both prepared identically.			
20 DISTRIBUTION/AVAILABILITY OF ABSTRACT <input checked="" type="checkbox"/> UNCLASSIFIED/UNLIMITED <input type="checkbox"/> SAME AS RPT <input type="checkbox"/> DTIC USERS		21 ABSTRACT SECURITY CLASSIFICATION	
22a NAME OF RESPONSIBLE INDIVIDUAL Dr. Alan H. Rosenstein		22b TELEPHONE (Include Area Code) (202) 767-4933	22c OFFICE SYMBOL NE

DEPARTMENT OF MATERIALS SCIENCE AND ENGINEERING
McCORMICK SCHOOL OF ENGINEERING AND APPLIED SCIENCE
NORTHWESTERN UNIVERSITY
EVANSTON, IL 60208

Annual Technical Report on

Tailored Interfaces for Metal-Matrix Composites-
Fundamental Considerations

to

Electronic and Solid State Sciences Division
Air Force Office of Scientific Research
Bolling Air Force Base
Washington, DC 20332
Attn: Dr. Alan H. Rosenstein
AF Grant No.: AFOSR-89-0043

For the Period
1 October 1989 to 30 September 1990

Principle Investigators

Morris E. Fine, Walter P. Murphy Professor of Materials Science and Engineering
Julia R. Weertman, Walter P. Murphy Professor of Materials Science and Engineering

31 October 1990

PROFESSIONAL PERSONNEL

Professor Morris E. Fine, Principal Investigator

Professor Julia R. Weertman, Principal Investigator

* John J. Blum, Ph.D. Student, Third Year Graduate Research Assistant

* Neil R. Brown, Ph.D. Student, Second Year Graduate Research Assistant

* Phillip A. Earvolino, Ph.D. Student, Second Year, AFOSR Fellow

* Rahul Mitra, Ph.D. Student, Second Year Graduate Research Assistant

* Resume at end of proposal.

SUMMARY

The objective of this research is to determine the interface properties needed for successful metal matrix composites and to learn how to achieve these properties. A number of factors have been selected for study. These are thermodynamic stability of the interface, nature of the bonding across the interface, energy and structure of the interface, and role of adsorption at the interface. a number of systems have been chosen to probe these factors; namely, Al/TiC, Al/ α -Al₂O₃, Al/MgAl₂O₄ (spinel), Al/Al₃(Ti_x, Zr_{1-x}), Mg/SiC, Mg/MgO, and Mg/Al₂O₃. Techniques for preparing all of these composites have been worked out, including mechanical alloying followed by extrusion, arc melting, and liquid metal infiltration into a preform of dispersed phase. Also, Mg alloy-SiC composites and Al-TiC have been obtained from Dow Chemical and Martin-Marietta, respectively. Microstructures of the resulting MMCs are presented and discussed along with studies of some of the interfaces using transmission electron microscopy. In comparison to Al/SiC, Al/TiC and Mg/SiC show no evidence of chemical reaction at the interface during processing. However, holding Al/TiC at 900°C for a long time did produce a reaction product at the interface which may be AlTi₃C. Al/MgAl₂O₄ (spinel) has superior mechanical properties to Al/Al₂O₃, both prepared identically. In material prepared by mechanical alloying, spinel particles are found inside grain boundaries. This indicates the former has a lower interfacial energy with Al.

STATEMENT OF WORK

Synthetic MMCs have a number of attractive features. It appears possible to design a composite material which meets specified criteria by a suitable choice of phases. However, whether or not the material actually is satisfactory depends in large part on the



Distribution/Availability Codes	
Dist	Avail and/or Special
A-1	

nature of the interface between the matrix and the other phase or phases. In this research a number of properties on the interfaces in MMCs which have a strong bearing on performance are under investigation. These properties include the thermodynamic stability of the interface region, the nature of the interfacial bonding, and segregation at the interface of a solute species as the result of Gibbs adsorption. It is the goal of this research to obtain basic information about those aspects of the interface which will permit the formulation of general principles to guide the tailoring of interfaces in MMCs in order to obtain optimum performance.

Interfaces in large part control the behavior of materials with a heterogeneous microstructure. Because of the complexity of interfaces, as well as the need for atomic resolution techniques to study them in detail, many questions remain about their structure, chemistry, and behavior under service conditions. Interfaces in a number of MMCs are to be investigated down to an atomic scale. The structure and chemistry are to be related to the behavior of material in the boundary region as well as to the composite as a whole.

INTRODUCTION

While synthetic MMCs have a number of attractive features, whether or not the material actually is satisfactory depends in large part on the nature of the interface between the matrix and the other phase or phases. The purpose of this research is to study, in as general a fashion as possible, properties of the interfaces in MMCs such as thermodynamic stability, the degree of coherency between the matrix and other phase lattices, the nature of the interfacial bonding, and solute segregation. The goal is to obtain basic information about the interface to guide tailoring of interfaces in MMCs to obtain optimum performance. Because of the complexity of interfaces, as well as the need for

atomic resolution techniques to study them in detail, many questions remain about their structure, chemistry, and behavior under service conditions. This study of interfaces aims to relate the structure and chemistry to the behavior of material in the boundary region as well as to the composite as a whole.

The main body of this report consists of four individual progress reports by the four Ph.D graduate students:

- I Mechanical Properties of Spinel and α -Alumina MMCs
By John J. Blum
- II Magnesium Metal Matrix Composites
By Neil R. Brown
- III Al/ $\text{Al}_3\text{Zr}_x\text{Ti}_{1-x}$ Metal Matrix Composite
By Philip A. Earvolino
- IV Study of Interface in Al/TiC Metal Matrix Composites
By Rahul Mitra

MODEL SYSTEMS UNDER STUDY

Model systems have been chosen to probe particular aspects of interfaces.

1. Chemical Control of the Reaction Zone at the Interface

The formation of Al_4C_3 and Al_2O_3 reaction zones in $\text{Al}/\text{SiC}(\text{SiO}_x)$ metal-matrix composites is well-known. These brittle interfacial regions are prime sites for crack initiation and cause low fracture toughness and ductility.

Three systems were selected to investigate the interfacial reaction zone structure and kinetics: Al/SiC , Al/TiC , and Mg/SiC . While the standard free energy of formation of Al_4C_3 is rather close to that of SiC , the free energy of formation of TiC is much lower and should be less likely to form a chemical reaction zone. Similarly, no reaction zone is expected in the Mg/SiC composite; however, elements present in Mg alloys may react with SiC .

2. Effect of the Nature of the Chemical Bond Across the Interface

The interfacial bond between a metallic matrix and an ionically bonded dispersoid is expected to be more ionic in character than the bond between a metallic matrix and an intermetallic particle. In the latter case the nature of the interfacial bond should be predominantly metallic. A metal-matrix composite with metallically bonded particles may have superior ductility and fracture toughness than an MMC with ionic or covalent interfacial bonding. To test this hypothesis, $\text{Al}/\text{Al}_3(\text{Ti},\text{Zr})$ will be investigated and compared to systems with oxide dispersoids, MgO , $\alpha\text{-Al}_2\text{O}_3$ and MgAl_2O_4 . The $\text{Al}/\text{Al}_3(\text{Ti},\text{Zr})$ system contains intermetallic particles and should represent MMCs whose interfacial bonds are primarily metallic in character. Also, the metal/ TiC interface may have more metallic character than the metal/oxide interface.

3. Coherent or Semi-Coherent versus Incoherent Interfaces

The degree of coherency of the interface in an MMC affects the strength, fracture toughness and microstructural stability at elevated temperatures. The particle/matrix interfaces in the magnesium alloy TiC composites are expected to be incoherent, since Mg is hexagonal and the dispersed phase is cubic. A coherent Al/MgAl₂O₄ interface seems possible since the lattice parameter of cubic MgAl₂O₄ is close to twice that of aluminum. With the proper processing treatment it is possible that coherent interfaces can be found in the Al/MgAl₂O₄ MMC but no such interface is expected with hexagonal α -Al₂O₃.

Semi-coherency vs. incoherency is being examined in the Al₃(Ti,Zr) system where coherent metastable cubic L1₂-structured precipitates may be formed. These have been extensively studied by us. The semi-coherent tetragonal DO₂₂ or DO₂₃-structured Al₃(Ti,Zr) phases are the stable phases in this system. An Al matrix MMC with the DO₂₃-structured Al₃(Ti,Zr) phase may be made by solidification and was shown to be ductile in previous research. It is possible that cubic L1₂-structured dispersoids may be made stable by alloying with transition metals.

4. Lowering Interfacial Energy by Chemadsorption

To the author's knowledge, chemadsorption has not been tried as a means of reducing interfacial energy to improve the fracture resistance of metal-matrix composites. Of course, if the technique is to be useful, the chemadsorption should not lead to interfacial embrittlement. The Al/Al₃(Ti,Zr) system also appears promising for the study of chemadsorption at the interface. The lattice registry between particles and matrix is a function of the Zr/Ti ratio in this alloy. As the alloy composition is varied, the driving

force for interfacial adsorption to reduce elastic strain energy should change.

PROGRESS

The research team consists of four graduate student research assistants, three supported on the AFOSR Grant and one by a DOD Fellowship. Their resumes are attached to this report.

The progress during the past year has been in developing improved sample fabricating techniques, structural studies and property testing. We have been fortunate in obtaining donated industrial assistance in material preparation. The systems under study are covered separately in the following section: I-IV.

I. Mechanical Properties of Spinel and α -Alumina MMCs

By John J. Blum

Initially, the possibility of a semi-coherent interface led to the choice of spinel as a dispersion strengthening agent in Al-based metal-matrix composites due to its lattice parameter which is approximately twice that of aluminum. For comparison with the spinel strengthened material, α -alumina, with its hexagonal structure was chosen to form a non-coherent interface. Material made by mechanical alloying disclosed that a better microstructure was obtained with spinel than with α -alumina in that the particle size was smaller and more uniformly distributed. This was due to greater reduction in particle size of spinel than α -alumina during mechanical alloying. Although the mechanical properties for the spinel MMC were quite good for oxide dispersed materials, a comparison between the intrinsic effect on mechanical properties of spinel and alumina particles was not possible since the final oxide particle sizes differed. Therefore, to better compare the two oxide dispersion strengthened materials, 25 volume percent Al-3 Mg composites with spinel or alumina dispersoids were prepared with larger initial spinel particle sizes than α -alumina particle sizes. The two MMCs were otherwise processed identically. Initial investigation into a low volume fraction of dispersoids in the Al-Spinel and Al-Alumina systems was conducted by Creasy et. al. [1] Later, mechanical property tests were conducted on the 10 vol% dispersoid MMCs by Blum et. al. [2] The effect of volume fraction is currently being investigated. Table 1.1 shows the initial particle sizes of the powders used in the fabrication of the 10 and 25 volume percent composites and the

processing schedules.

After mechanical alloying, the powders are vacuum degassed at 350°C to remove any adsorbed gases and then pressed into billets. Later, these billets are preheated to 400°C and then hot-extruded with a reduction ratio of $\approx 20:1$. Lastly, specimens are machined directly from the extruded rod in either the as-received or annealed condition. Figure I.1 is a schematic diagram of the fabrication process.

Recent investigations of the formation of spinel on alumina particles in Al-Mg systems has introduced the possibility of partial coherency in the Al-alumina composite. [3] Therefore, testing in the as-received as well as annealed state is being performed to relate the nucleation and growth of the interfacial spinel with mechanical properties as a function of annealing time.

RESULTS

Compression tests were performed on an Instron Model 1250 testing machine equipped with a vacuum furnace and axial extensometer. The 10 volume percent composites were tested in the as-received condition in strain control at strain rates varying from 10^{-1} to 10^{-6} per second at 20, 225, 325 and 425°C. The results are graphically presented in Figure I.2. The Al-spinel material is approximately 30% stronger than the Al-alumina material at comparable temperatures and strain rates. In order to identify the differences which yield the different strengths noted, TEM investigations into grain size and particle size were undertaken. Hundreds of TEM micrographs were taken to find an average grain size in both the longitudinal and transverse directions with respect to the extrusion directions. The grain sizes were in the submicron range. (Table I.2) The Al-3 Mg spinel MMC's grain size was smaller than that of alumina composite, which may

account for some of the strength difference. However, particle-dislocation interaction was expected to be the major strengthening mechanism. TEM investigations of the particle size was undertaken and showed that the Al-Spinel material exhibited a bimodal distribution of particles while the particle distribution in the Al-Alumina composite was primarily unimodal. Particle sizes after processing are shown in Table I.1. Furthermore, many spinel particles were distributed in the grains while the alumina particles were primarily at grain boundaries. This may indicate that the spinel matrix interfacial energy is lower than that for α -alumina.

A comparison of the 10 volume percent Al-Spinel and Al-Alumina with pure aluminum and dilute solutions of Al-Mg is shown in Figure I.3. In order to compensate for temperature, strain rate is normalized by bulk diffusivity of aluminum and stress is normalized by temperature corrected Young's Modulus. While the 10 volume percent composites show strengths slightly greater than Al-Mg alloys at intermediate (225°C) temperatures, the oxide dispersed materials are much stronger at temperatures approaching $3/4 T_m$ (425°C). Upon close inspection, both composites show a temperature dependent threshold stress. An extrapolation of $(\epsilon/t)^{1/n}$ vs. σ to zero strain rate yields threshold stress as a function of temperature for both composites. Figure I.4 is such a plot with $n=2$ which yields the best correlation factor. A normalized threshold stress can then be plotted against the inverse of temperature to obtain an activation energy for creep. Figure I.5 shows that there are different activation energies at different temperatures. Further testing at other elevated temperatures will shed more light on this phenomenon.

The newly received 25 volume percent composites have been tested at room

temperature and 225°C. Initial testing has shown the strengths of both materials to be near 700 MPa at 20°C and 350 Mpa at 225°C. Further compression tests at higher temperatures are currently underway. Additionally, investigation of particle and grain sizes will be undertaken in the near future.

In addition to compression tests, modulus measurements using a acoustic resonance technique were performed. Figure I.6 shows moduli for both composites as a function of volume fraction. Values for 100% alumina and spinel were obtained from Hertzberg [8]. Additional modulus tests as a function of annealing period are planned. Information relating modulus to the integrity of the matrix/oxide bond may be shown.

Dilatometry has been performed on the 10 volume percent materials. The coefficients of thermal expansion are lower than that for Al 3 wt. pct. Mg matrix material tested identically. Coefficients for both the Al-Spinel and Al-Alumina composites are $24\mu\text{m}/\text{m}/^\circ\text{K}$ while the matrix material's CTE is $27\mu\text{m}/\text{m}/^\circ\text{K}$. The CTEs are determined in the range 200 - 400°C. Subsequent cycling of the materials up to 5 cycles failed to change the CTEs significantly. Cycling up to 100 cycles is planned in order to detect any interfacial changes. No dilatometry has yet been performed on the 25 vol. pct. composites.

SUMMARY

A greater reduction of particle size during mechanical alloying was observed for the spinel particles. Initial particle sizes were $\approx 1\text{-}2\mu\text{m}$ for alumina and $\approx 3\mu\text{m}$ for spine!. (Table I.1)

Grain sizes for both 10 v/o composites range between 0.1 and 1 μm . (Table I.2)
The smaller grain size of the spinel MMC is attributed to a finer dispersion of spinel than

that of alumina.

Al-Spinel was 30% stronger than Al-Alumina at all temperatures. (Figure 1.2)

Much greater high temperature strengths were observed for both composites in comparison to published results for pure aluminum and dilute aluminum - magnesium alloys. (Figure 1.3)

Multiple activation energies for creep are expected from high temperature compression tests performed at slow strain rate tests. This result implies a change in deformation mechanism with temperature. (Figure 1.5)

The modulus of Al-Spinel and Al-Alumina 10 vol. pct. composites is approximately 15% higher than that of Al 3 wt. pct. Mg matrix material. (Figure 1.6)

Linear coefficients of thermal expansion were reduced by approximately 11% for both composites compared with Al 3 wt. pct. Mg. Thermal cycling failed to change the observed CTEs.

CONCLUSIONS

Al-Spinel and Al-Alumina composites are materials well suited for applications up to 400°C due to their improved high temperature strengths, high modulus and improved coefficients of thermal expansion.

Due to the extensive break-up of spinel particles during mechanical alloying, Al-Spinel is ~30% stronger than the Al-Alumina composite at all temperatures implying that composite strength is proportional to the inverse of the particle interspacing. This result is compatible with current theories concerning deformation of materials containing hard, unshearable particles.

Larger volume fractions of dispersed oxides will yield even stronger composites. Work currently underway on 25 vol. pct. Al-Spinel and Al-Alumina materials has yielded compressive strengths up to 700 MPa (\approx 100 ksi) at room temperature.

REFERENCES

- 1 T. Creasy, J. R. Weertman and M. E. Fine, "Aluminum Alloy with Spinel for Oxide Dispersion Strengthening", Dispersion Strengthened Aluminum Alloys, Eds. Y.-W. Kim and W. M. Griffith, The Minerals, Metals and Materials Society, 1988.
- 2 J. J. Blum, J. R. Weertman and M. E. Fine, to be submitted to Scripta Metall.
- 3 C. Horng, A. Lin and K Liu, "Formation of $MgAl_2O_4$ in Al_2O_3 /Al-4%Mg Composites", TMS Fall Meeting, Detroit, 1990
- 4 I. S. Servi and N. J. Grant, *Trans. Am. Inst. Min. Engrs.*, **191**, 909 (1951).
- 5 H. Luthy, A. K. Miller and O. D. Sherby, *Acta Metall.*, **28**, 169 (1980).
- 6 H. Oikawa, K. Sugawara and S. Karashima, *Trans. Japan Inst. Metals*, **19**, 611 (1978).
- 7 K. Murty, G. A. Mohamed and J. E. Dorn, *Acta Metall.*, **20**, 1009 (1972).
- 8 R. W. Hertzberg, Deformation and Fracture Mechanics of Engineering Materials, John Wiley & Sons, New York, pp. 8-14 (1976).

Table I.1: Processing schedules, initial particle sizes and final particle sizes for 10 and 25 volume percent mechanically alloyed composites.

MATERIAL	VOL/O	SCHEDULE	INIT. PARTICLE SIZE	FINAL PARTICLE SIZE
SPINEL	10	1 HR.	$\approx 3\mu\text{m}$	Gr. Bndry. - $0.1\mu\text{m}$ Gr. Inter. - 70 nm
ALUMINA	10	30 MIN	$\approx 1\text{-}2\mu\text{m}$	$0.4\mu\text{m}$
SPINEL	25	8 HRS.	$\approx 3\mu\text{m}$	-----
ALUMINA	25	8 HRS.	$\approx 0.2\mu\text{m}$	-----

Table I.2: Grain sizes and grain aspect ratios for 10 volume percent Alumina and Spinel composites.

MATERIAL	GRAIN SIZE		GRAIN ASPECT RATIO
	LONGITUDINAL	TRANSVERSE	
ALUMINA	0.96	0.77	1.25
SPINEL	0.73	0.35	2.09

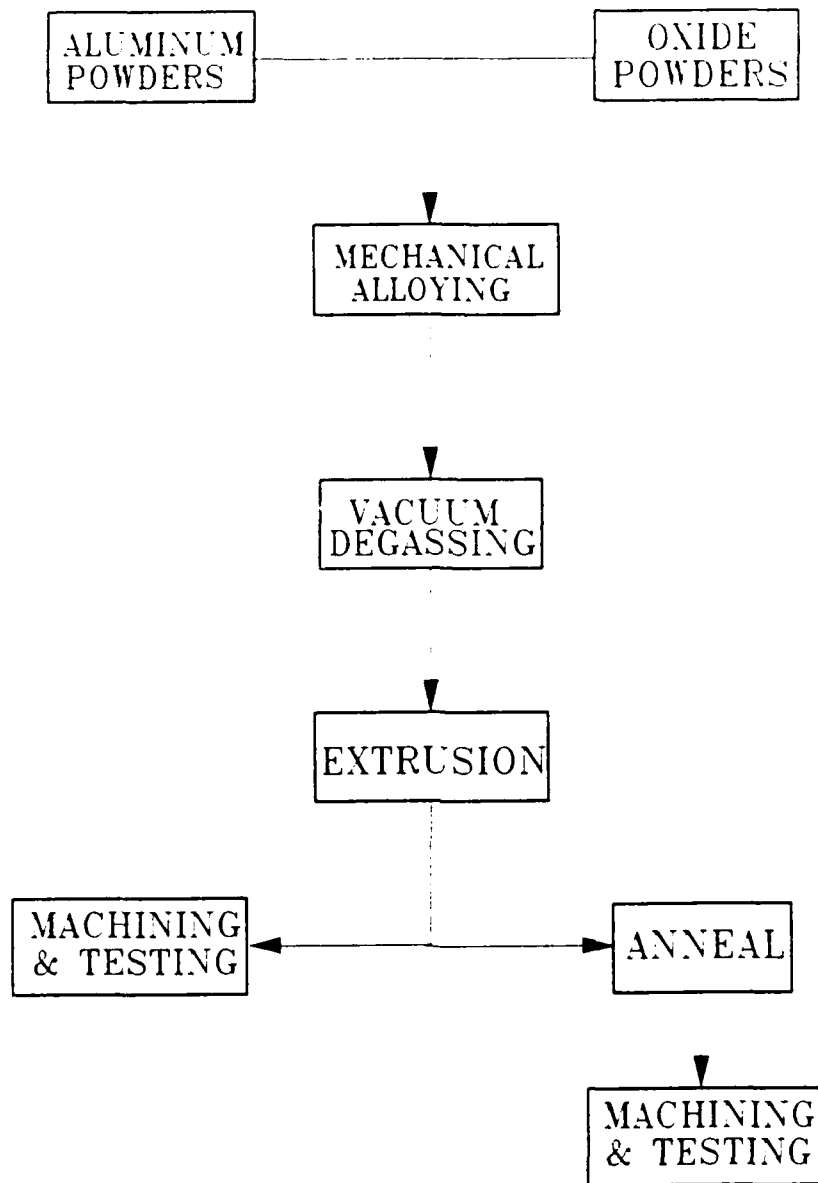


Figure I.1: Schematic diagram of the Al-Spinel and Al-Alumina composite processing schedules.

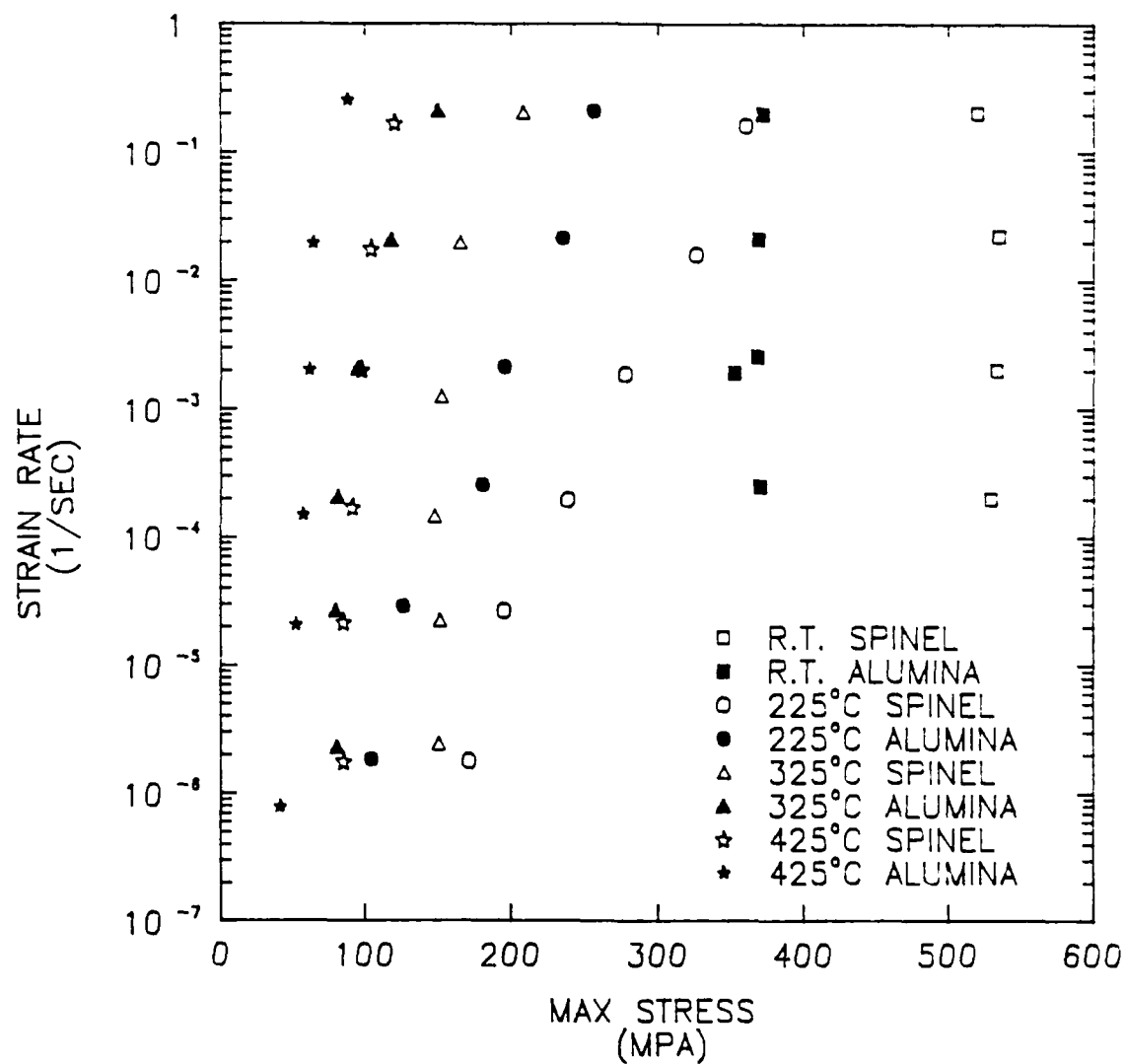


Figure I.2: Compressive stress as a function of strain rate and temperature for 10 volume percent Al-Spinel and Al-Alumina composites.

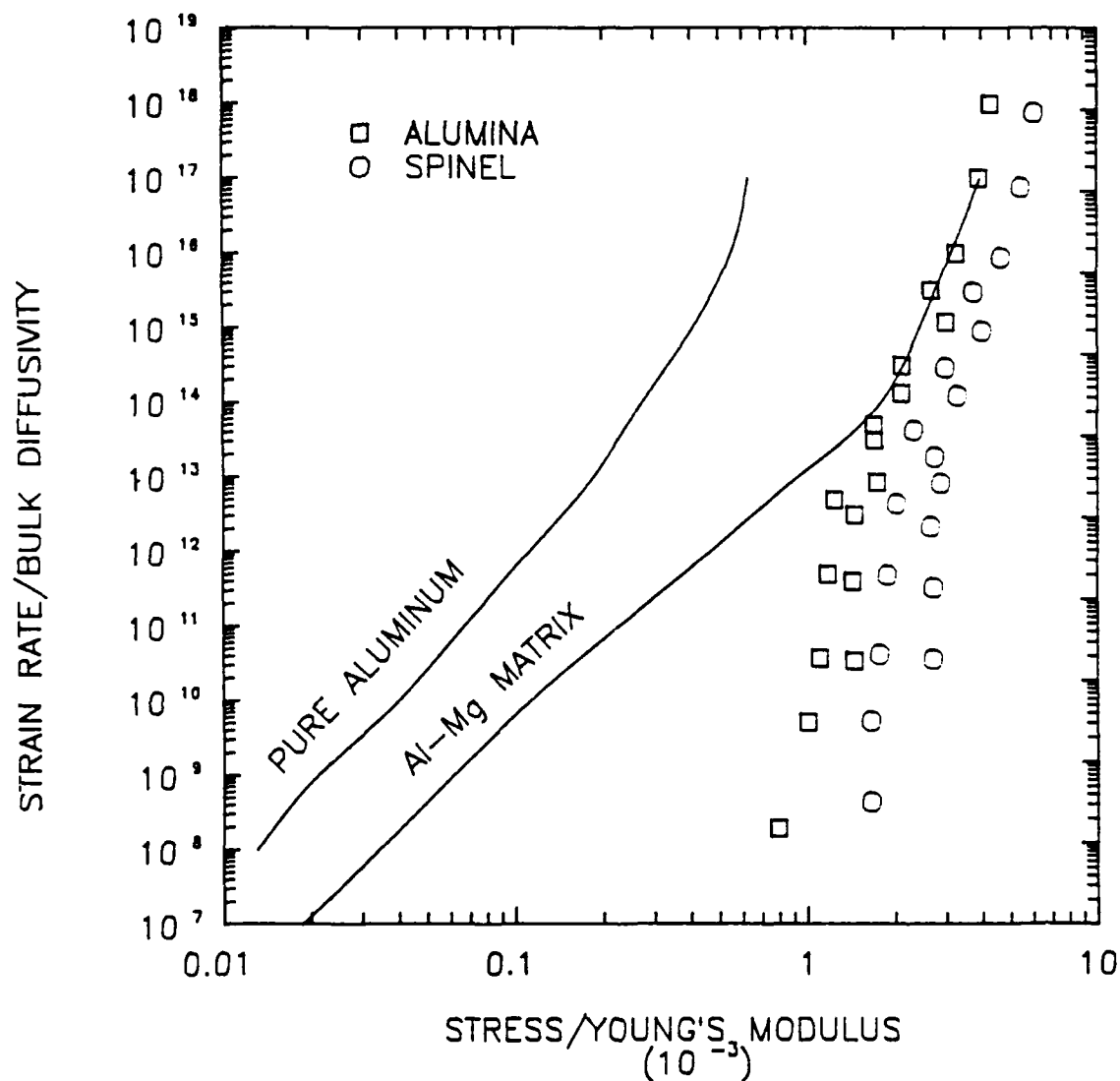


Figure I.3: Comparison of temperature compensated plots of strain rate normalized by bulk diffusivity of Al versus stress normalized by Young's modulus for 10 vol. pct. mechanically alloyed Al-Spinel and Al-Alumina composites with published data for pure aluminum and Al-Mg, the matrix material of the composites. Data for pure aluminum from [4,5] and Al-Mg (2-5%) from [6,7].

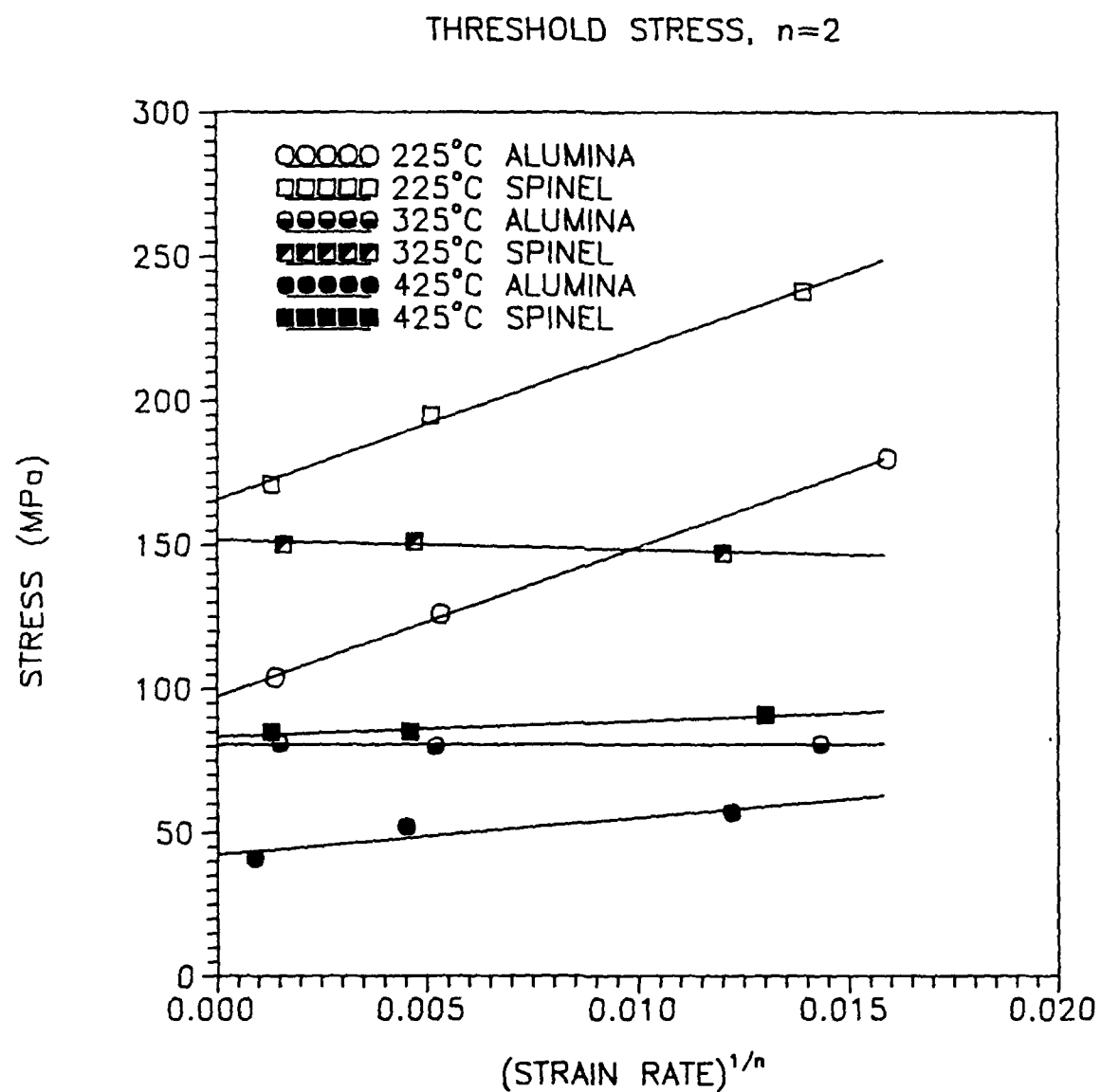


Figure 1.4: Extrapolation of $(\epsilon/t)^{1/n}$ to zero for derivation of threshold stresses.

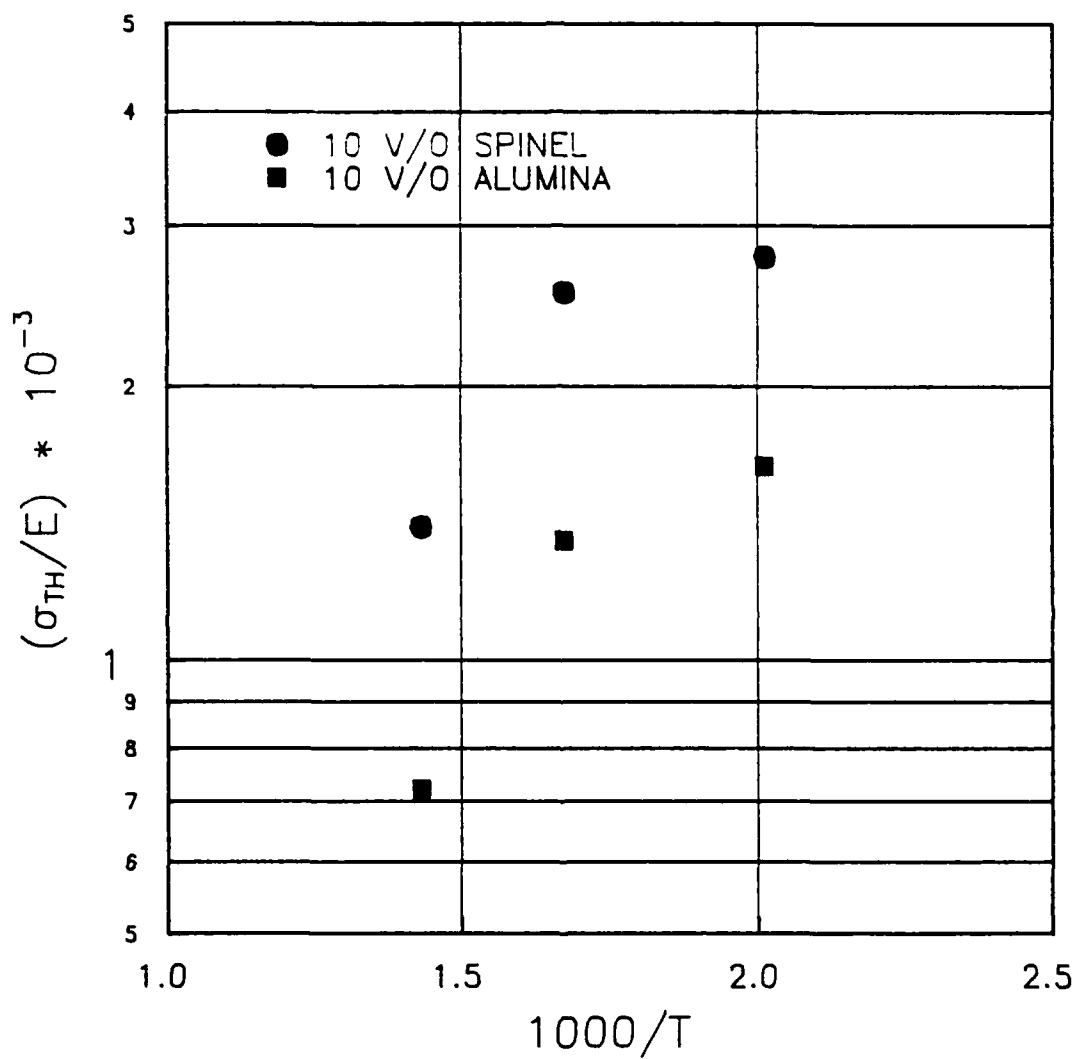


Figure I.5: Activation energies Q_1 and Q_2 derived from threshold stresses as a function of temperature.

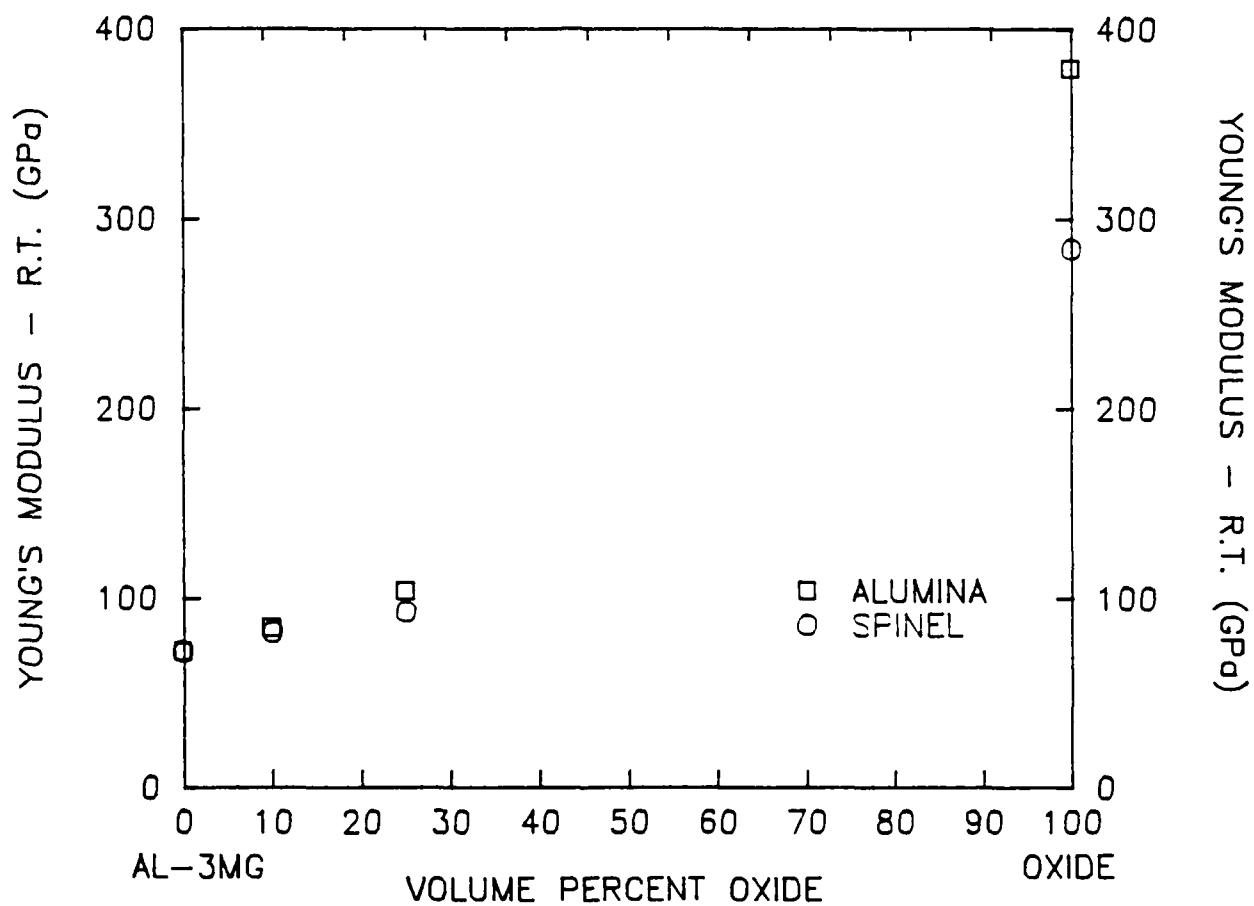


Figure I.6: Plot of modulus versus volume percent oxide contained in Al-Spinel and Al-Alumina composites. Values for pure oxides obtained from Hertzberg. [8]

II.

Magnesium Metal Matrix Composites

by Neil R. Brown

The purpose of this report is to describe the research progress made on magnesium metal matrix composites. Originally Mg / SiC, Mg / MgO and Mg / Mg₂Si were selected for study. For reasons described below, Mg / Al₂O₃ has replaced the study of Mg / Mg₂Si. The three materials of interest still satisfy the goal of the project of studying different bonding types and interfaces in metal matrix composites. The first, Mg / SiC, should not exhibit a reaction zone, since Mg does not form a stable carbide and SiC has a much lower free energy of formation than Mg₂Si. Similarly, Mg / MgO should not form a reaction zone since the reaction zone would itself be MgO. Also, the Mg / MgO composite should exhibit more ionic bonding than the Mg / SiC composite due to the formation of Mg-O bonds across the interface. Finally, Mg / Al₂O₃ is known to form a reaction zone. There is some controversy as to whether the reaction zone is MgO [1] or spinel (MgAl₂O₄) [2,3]. This should be readily determined by TEM observations of composites and high resolution analytic microscopy.

As mentioned above, the study of Mg / Mg₂Si has been replaced by the study of Mg / Al₂O₃. This was done because the Mg₂Si was found to all segregate to the grain boundaries. With silicides present at the grain boundaries, the material was too brittle to be of practical interest. In an attempt to recrystallize the material, it was hot rolled at 400°C to a thickness reduction of 25% and then annealed for 5 hours at 400°C. The silicide remained at the grain boundaries, with the only noticeable effect being enlargement of the silicides. Further attempts to roll the material at lower temperatures failed due to the extreme brittleness of the material as did further rolling at elevated temperatures.

Originally, in house samples were made by pulling molten magnesium and stirred in particulate into dry quartz tubes. This seemed to give nice specimens, but

over time they were found to pit and corrode under standard atmospheric conditions probably due to a very fine dispersion of flux inclusions. Thus for safety reasons, a new method of making in house samples had to be found. As mentioned in last year's report, arc melting and powder metallurgy are not suitable. Finally, the use of liquid metal infiltration was decided upon. In this method, magnesium is placed over the particulate and then melted at 720°C under a flowing argon atmosphere and allowed to flow into the space between the particles or fibers. This method is particularly suited for magnesium due to its high vapor pressure, low melting point and high reactivity allowing for wetting [4]. Dupont Inc. has used this method to make Mg / Al₂O₃ fiber composites [1]. Samples of Mg / MgO that are suitable for transmission electron microscopy have been produced. This method should allow for production of all of the necessary samples, that cannot be obtained commercially, for detailed TEM studies.

Several commercial materials are also under study. Dow Inc. in Freeport, Texas has furnished to the research a Mg-6%Zn (known as Z6 alloy) / 20 v% 1000 grit SiC composite and a Mg-3% rare earth (cerium mischmetal)-1%Mn (known as EM31 alloy) / 3 v% 1000 grit SiC composite. Also, they are currently sending an EM31 / 3v% Al₂O₃. These materials were produced by a proprietary liquid casting method followed by extrusion. This produces a very uniform distribution of particles and very good mechanical properties (see below). The particles are aligned along the longitudinal extrusion direction. Through TEM and SEM microscopy, done at Northwestern, the particles were found to be approximately 6x1x1µm in size, with the longest direction along the extrusion direction. This should provide for different material properties between the longitudinal and transverse directions. Also of note is that these alloys are casting alloys that have been extruded at an 18:1 ratio. Unfortunately Dow did not make any pure matrix materials under the same conditions as the composites. Thus the matrix properties are not known for these materials. The nanoindenter at Sandia National Laboratories in Albuquerque, New Mexico will be used in December to

determine these properties. This instrument can vary loads from 0.05- 12 grams and achieve indents at a spacing of approximately one micron. This will allow for the determination of the properties as a function of distance from the particles. This should be of interest due to the large residual strains around particles caused by thermal mismatch between the ceramic and the metal. Possible effects of these strains are work hardening of the matrix and increased aging response^[5] in the vicinity of the particles. Further work on these materials includes the same studies but under various heat treatments.

Several of the above mentioned effects have already been observed through the use of transmission electron microscopy. All TEM samples were prepared by mechanical thinning followed by ion milling with the use of a liquid nitrogen stage. First of all, in Figure [1] several small precipitates can be seen near the interface of silicon carbide particles in the EM31 matrix. These precipitates were present near a number of the particles but were not found anywhere else in the matrix. These will be identified through the use of analytic microscopy and selected area diffraction. They are probably a magnesium cerium intermetallic since manganese does not form an intermetallic with magnesium. Second, through the use of selected area diffraction with the area bisected by the interface an unknown finely grained crystalline phase with random orientation was found. This compound produces very sharp diffraction rings indicating its fine grain structure. This same phase was not found in the matrix. This phase is unknown, but by examination of the d-spacings indicated by the diffraction pattern it is not Mg, C, SiC or Mg₂Si. The composition of this unknown phase will be determined through further diffraction work and analytic TEM.

Figures [2,3] show the sharp interface present in the EM31 / SiC composite. Notice that there are no gaps or voids near the interface and that the interface was not preferentially milled as is evident by the presence of magnesium on either side of the SiC particles followed by holes. In Figure [3] a broken SiC particle with void free

magnesium surrounding the broken off area provides further evidence of the strong interface between the two materials. This research confirms the prediction that there would not be an embrittling reaction zone between Mg and SiC.

In conjunction with microscopy, mechanical testing is also underway. Arsenault^[6] proposed a mechanical test that provides a lower bound for the bond strength of a particulate reinforced composite. The reader is referred to Rahul Mitra's section of this report for an explanation concerning this procedure. Five tensile tests on the EM31 3 %SiC composite were run at strain rates varying from 2.38×10^{-5} , 2.38×10^{-4} and 4.76×10^{-4} /s and crosshead speeds of .05, .5 and 1 mm / minute. These samples were oriented along the longitudinal direction. As mentioned earlier with the highly aligned particles it will also be necessary to do these tests for the transverse direction. This will allow for comparison between two different area fractions. All of the samples failed in a brittle manner with just a slight turnover in the *stress strain curve*. Figures [4,5,6] show fracture surfaces of the samples. In each test no debonding of the particles was noted, with the fracture path either through the particles or around them. The samples broke at a failure stress of 283 MPa and a coefficient of variation (standard deviation divided by the mean) of only 0.038. This low coefficient of variation is proof of the identical nature of failure and also indication of material uniformity. Based upon Arsenault, this data provides for a maximum triaxial stress of 730 MPa. Since the failure mechanism was matrix and particle failure this test is indicative of their combined strength and not that of the larger interface strength. This figure is surprisingly high when compared to the tensile strength for AZ61-F of 230 MPa.^[7] This alloy is useful for comparison because it is the strongest, non heat treated wrought alloy. Also of note is that these results were for the as received material and will be repeated for differing heat treatments.

Further work in this area includes wire cutting of the stressed specimens followed by an anneal to equilibrate any voids that may have formed between the

particle and the matrix. Through the use of TEM the contact angle of the voids can be measured. With this information and the surface energies of the particulate and the matrix, the work of adhesion can be measured.

In conclusion, through the work that has been done so far, and the work that is planned for the future, a good understanding of the interfacial properties of these three magnesium metal matrix composites should be reached. And with this information, some insight should be gained into the effect of various interface types upon the mechanical properties of metal matrix composites.

References

1. M. Pfeiffer, J.M. Rigsbee, K. K. Chawla "The Interface Microstructure in Alumina Fiber/ Magnesium Alloy Composites", Journal of Materials Science v 25,1990 p 1563-7
2. J. Nunes, E.S.C. Chin, J.M. Slepetz and N. Isangarakis International Conference on Composite Materials, ICCM-V Conference Proceedings (Pergamon, Oxford, 1985) p 723
3. E.S. C. Chin MS Thesis, Brown University, Providence Rhode Island (1983)
4. T. Crisafulli, American Metal Market / Metalmarketing News, May 27, 1985
5. B. Mikucki, "Heat Treatment of Mg-Zn Alloy Reinforced with Silicon Carbide Particulate", Fundamental Relationships Between Microstructure And Mechanical Properties of Metal Matrix Composites, The Minerals Metals and Materials Society,(1990)
6. Y. Flom and R.J. Arsenault, Material Science and Engineering, v.77, 1986 p. 191
7. ASM Handbook volume 2, 9th Edition p. 528

Figures

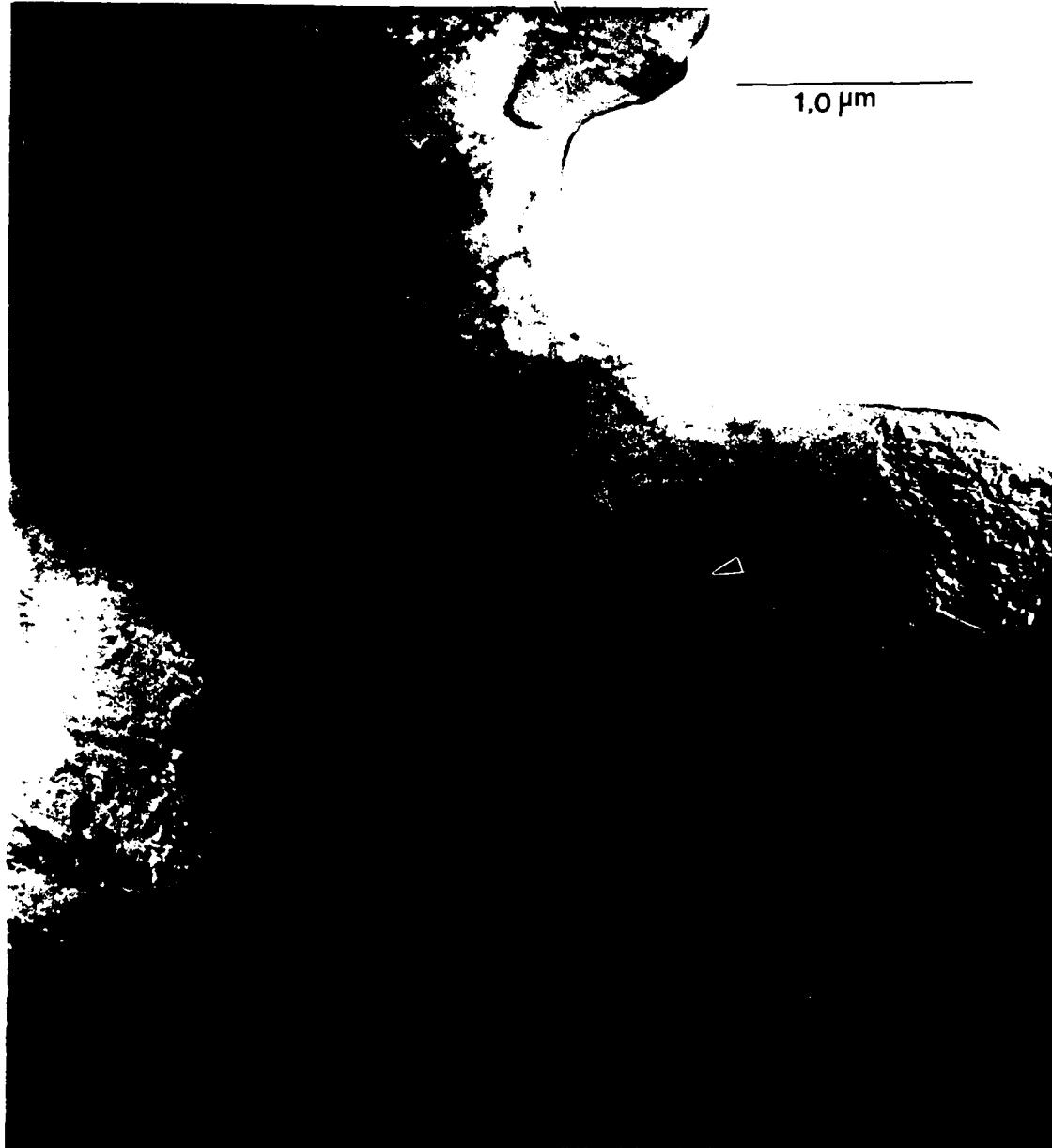


Figure 1. TEM micrograph of magnesium EM31 SiC Composite.
Several small precipitates are observable near the SiC / Mg
interface.

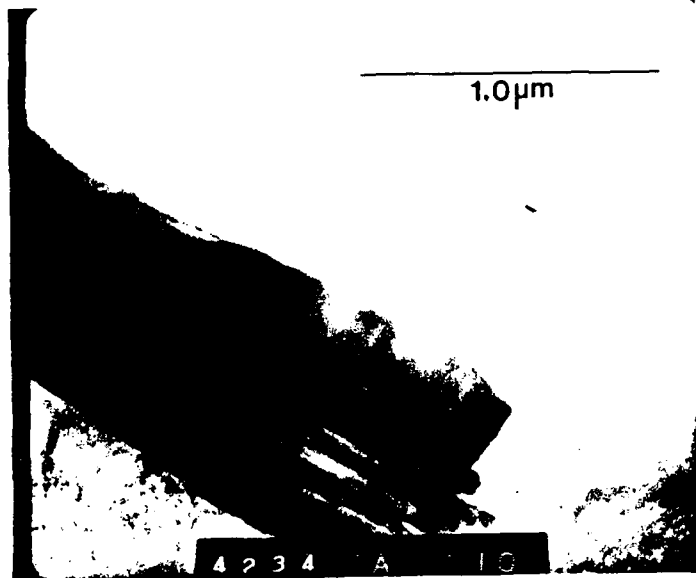


Figure 2. TEM micrograph of EM31 / SiC composite

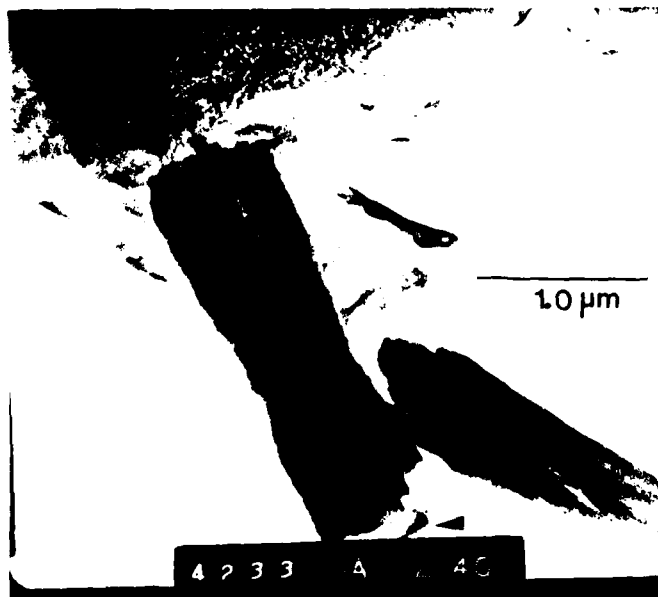


Figure 3. TEM Micrograph of EM31 / SiC composite. Void free magnesium surrounds the broken SiC particles.



Figure 4. SEM Micrograph of fracture surface of EM31 / SiC composite.
No particle debonding is evident.

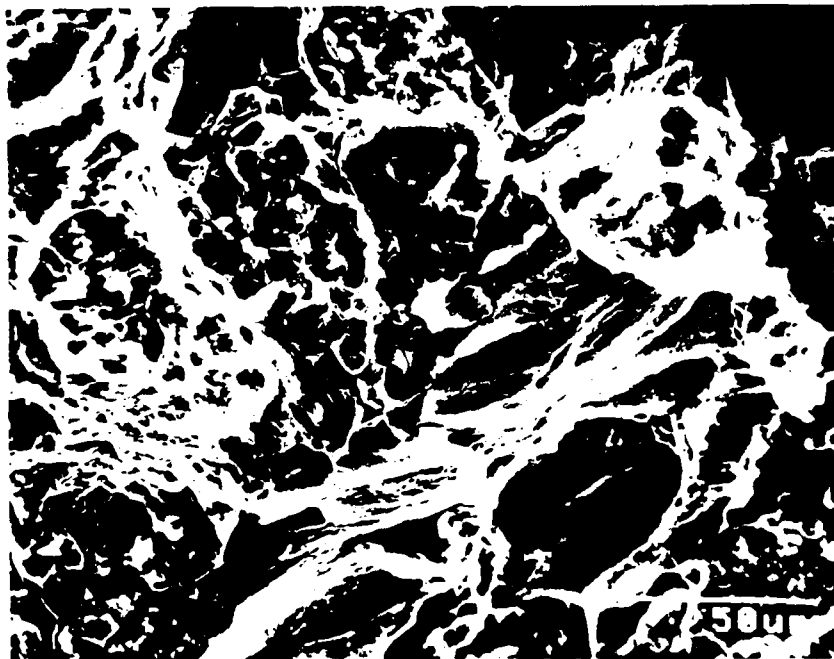


Figure 5. SEM Micrograph of fracture surface of EM31 / SiC composite.

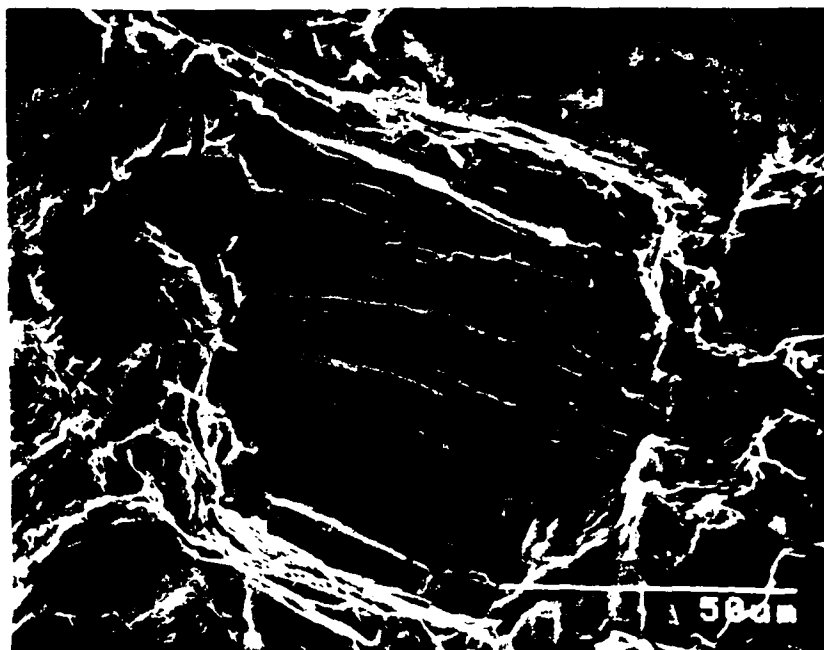


Figure 6. SEM Micrograph of fracture surface of EM31 / SiC composite.

III.

Al/Al₃Zr_xTi_{1-x} metal matrix composite

by

Philip Earvolino

Samples of the Al/Al₃Zr_xTi_{1-x} metal matrix composite have been prepared by arc-melting under an argon atmosphere. The melted buttons are flipped ten times to insure compositional homogeneity. The drawbacks of this method are twofold: porosity in the as-cast materials is high, in some cases as much as 25%; and, the largest sample which can be produced with the available apparatus weighs 12g. The intermetallic particles in the as-cast structure are needle-like; in a composite with 15 volume percent particles, the largest ones may be over 400 μm long but only 10 μm wide (see Figure III.1). They are tetragonal, of the DO₂₃ structure, as confirmed by diffractometry.

The arc-melted composite has shown considerable ductility, in spite of the porosity. An Al-Al₃Zr_{0.25}Ti_{0.75} (15v/o) has been hot-pressed (500 °C) to a final reduction of 59% and then cold-rolled to 99.74% total reduction (a thickness of 26 μm). By folding this foil and rolling it, an effective reduction of 99.983% has been achieved. After this extreme deformation, particles have been broken up severely: the dimensions of these smaller particles are approximately 15 μm by 5 μm .

Other samples, supplied by Lockheed, show a quite different microstructure than those prepared by arc-melting. These are in the form of melt-spun ribbons, approximately 2 mm wide and 50 μm thick. Due to the extreme cooling rates obtained in the melt-spinning process, the intermetallics

do not precipitate in the stable tetragonal form. Instead, they form spherical metastable $L1_2$ particles.

Transmission Electron Microscopy

An arc-melted $\text{Al-Al}_3\text{Zr}_{0.75}\text{Ti}_{0.25}$ (15v/o) sample was prepared for microscopy as follows. The sample was hot-pressed (500°C) to a reduction of 60% and then cold-rolled to a thickness of $120\text{ }\mu\text{m}$, representing a total reduction of 98.8%. From the resulting sheet of material, 3mm discs were cut on an electric discharge machine. These discs were then polished on 600 grit paper to a final thickness of $60\text{ }\mu\text{m}$. Finally, these were jet polished using an etchant of 2.7% perchloric acid (70%), 36% n-butyl alcohol, and 61% methyl alcohol, by volume at a temperature of -27°C . A Fischione polisher was used; the polishing conditions were 14 V and 8 mA. As this solution is specific for the intermetallic, the Al matrix was still thick and was thinned further by argon ion-milling at an incidence angle of 10° for one hour.

Figure III.2 is a TEM micrograph of the sample prepared above. The particle/matrix interface appears to be sharp and continuous. The diffraction pattern of the particle is also included (Fig. III.3).

Melt-spun samples supplied by Lockheed have shown initial promise. These have been prepared for TEM examination by cold-rolling to a thickness of $26\text{ }\mu\text{m}$ (a reduction of 50%), followed by polishing on 800 grit paper to a final thickness of approximately $20\text{ }\mu\text{m}$. Both of these procedures helped to reduce the surface roughness on the last-to-freeze side of the ribbon. 3 mm discs were punched out of the resulting ribbons and were jet polished in an etchant of 25% (by volume) nitric acid in methyl alcohol at a temperature of -39°C . A Struers double jet polisher was used; the operating conditions were 6 V and 12 mA.

Microscopy of one of these samples shows that spherical $L1_2$ particles have indeed formed; their diameters are in the range 15-20 nm. Another sample, however shows that the particles have tetragonal shape. Presumably, these are in regions of the ribbon exposed to far slower cooling rates than those which produce the metastable particle structure.

Matrix Strength

The matrix strength in the $Al/Al_3Zr_xTi_{1-x}$ system was determined using a method first described by Arsenault ¹. This approach, which was developed to provide an estimate of interfacial strength, will be described in detail in section IV. For the present study, fracture of the composite occurred in the matrix. Thus, a value for *matrix* strength is obtained. Two 12g samples were prepared by arc-melting: $Al-Al_3Zr_{0.25}Ti_{0.75}$ (3v/o) and $Al-Al_3Zr_{0.5}Ti_{0.5}$ (3v/o). They were swaged to a final diameter of 0.312 in (a reduction in cross-sectional area of 80%). Each of these rods was then electric discharge machined to produce specimens for tensile testing. Specimens were tested in tension to fracture on an Instron model 1125 machine. The cross-head speed was 10^{-3} in s^{-1} .

By determining the stress at fracture, a lower bound value for the interfacial strength may be obtained; the actual value is either higher or equal to this. The average value for the $Al-Al_3Zr_{0.25}Ti_{0.75}$ (3v/o) system was 411 MPa; for the $Al-Al_3Zr_{0.5}Ti_{0.5}$ (3v/o) system, the value was 442 MPa. These strengths are in the same range as those found by Mitra, who also tested a composite with a matrix of pure Al (see section IV). Although these strengths are lower than those found by Arsenault, his values are characteristic of a much stronger matrix, an Al 6061 alloy. SEM micrographs of the fracture surface are indicative

¹Y. Flom and R.J. Arsenault, *Mater. Sci. and Eng.*, **77**, 191 (1986).

of ductile fracture (Figure III.4). They do *not* show fracture at the particle-matrix interface; hence, a value for the strength of the interface can not be determined explicitly.

Elastic Modulus

The elastic moduli of composites of varying compositions were determined by a dynamic method. The modulus of a material is related to the resonant frequency of a displacement wave travelling through it by the relation:

$$E = 4L^2\rho f_n^2/n^2 \quad (III.1)$$

where L is the length of the sample, ρ is its density, f_n is its resonant frequency, and n is the number of zero-displacement nodes in the sample (for this experiment, assumed to equal one). If the material is cut in the form of a rectangular slab and clamped at one end to a piezoelectric crystal of known resonant frequency, then the resonant frequency of the slab of material will be given by:

$$f_s = f_c + (M_x/M_s)(f_c - f_x) \quad (III.2)$$

where f_s is the resonant frequency of the material sample, f_c is the resonant frequency of the composite system, M_x is the mass of crystal, M_s is the mass of the sample, and f_x is the resonant frequency of the crystal².

The modulus values obtained from this method are plotted against the fraction of intermetallic in the composite (Fig. III.5 and Fig. III.6). The line shown

²M. E. Fine, *ASTM Special Technical Publication*, 129, 43 (1952).

is the modulus predicted by the rule of mixtures, where the theoretical value is a weighted average of the moduli of the component materials in the composite. Presumably, weak or discontinuous interfaces will lead to lowering of moduli values; hence, greater deviation from the rule of mixtures. Plots are given for two different composite systems: Al-Al₃Zr_{0.5}Ti_{0.5} and Al-Al₃Zr_{0.25}Ti_{0.75}. All of the samples tested were hot-pressed and cold-rolled to a total reduction of approximately 80%. Although this breaks up particles and partially destroys the native interface, the cold-working was necessary to reduce porosities to values where their effect upon modulus was negligible. Indeed, modulus values for as-cast samples were shown to decrease in a roughly linear (correlation coefficient of 0.92) fashion with porosity fraction (Fig. III.7).

Future Plans

High resolution microscopy (HREM) will be performed on the melt-spun ribbon samples. In particular, the coherency of the particle-matrix interface must be determined. For the L₁₂ particles, samples have been thinned sufficiently for high resolution work. The DO₂₃ particles present in the arc-melted samples, however, will need to be thinned by a combination of electropolishing and ion milling for HREM analysis.



Fig. III.1. Al-Al₃Zr_{0.5}Ti_{0.5} (15 v/o). Arc-melted sample.



Fig. III.2. TEM micrograph of Al-Al₃Zr_{0.75}Ti_{0.25} (15 v/o). 98.8% reduction. Arrows indicate particle-matrix interface.

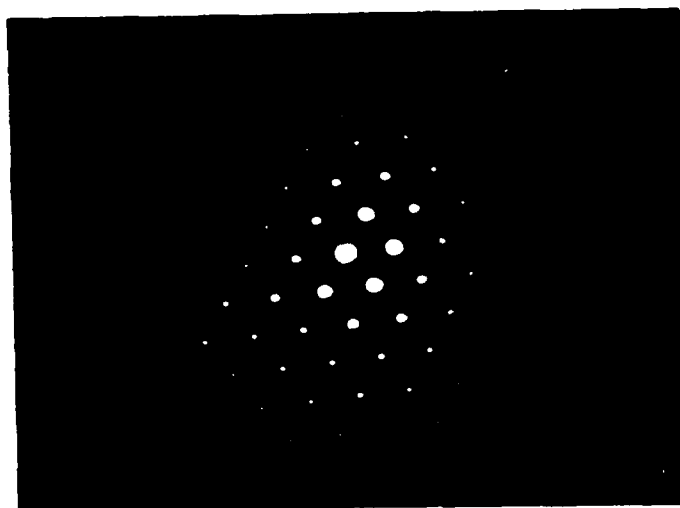


Fig. III.3. Electron diffraction pattern of Al-Al₃Zr_{0.75}Ti_{0.25} (15 v/o).

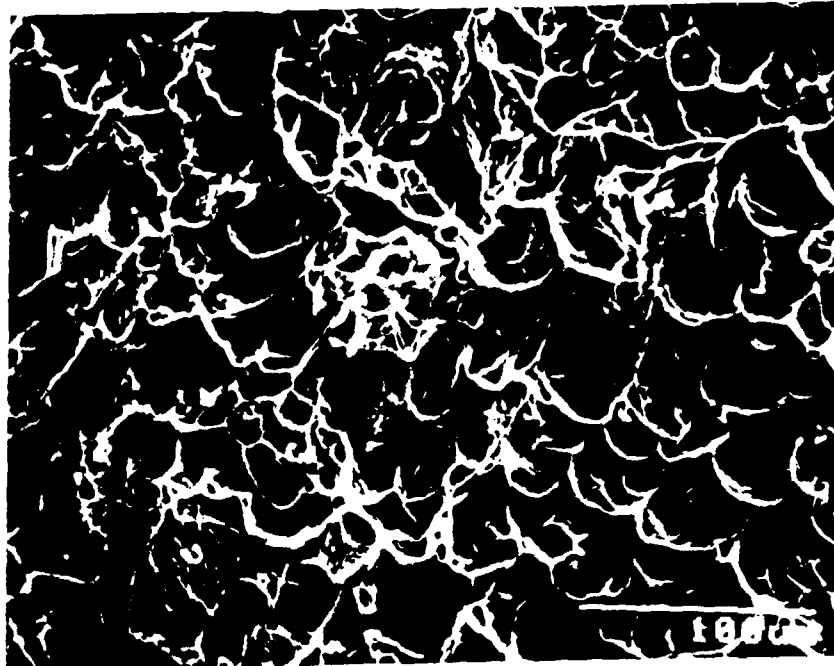


Fig. III. 4. Al-Al-Al₃Zr_{0.25}Ti_{0.75} (3 v/o) tested in tension to fracture.

Fig. III.5. Young's Modulus vs. volume percent precipitate
 $\text{Al}_3\text{Zr}_{.5}\text{Ti}_{.5}$

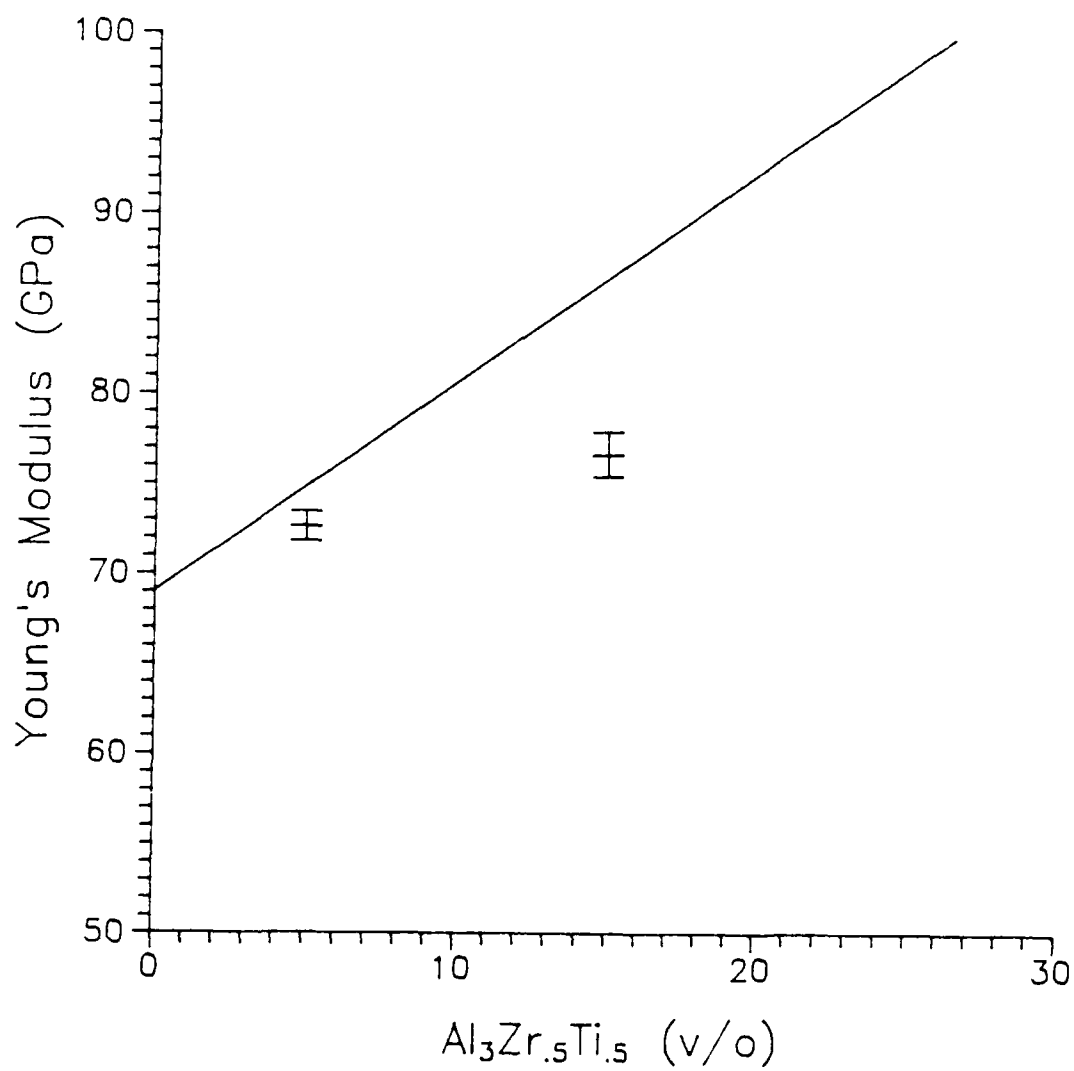


Fig. III.6. Young's Modulus vs. volume percent precipitate
 $\text{Al}_3\text{Zr}_{0.25}\text{Ti}_{0.75}$

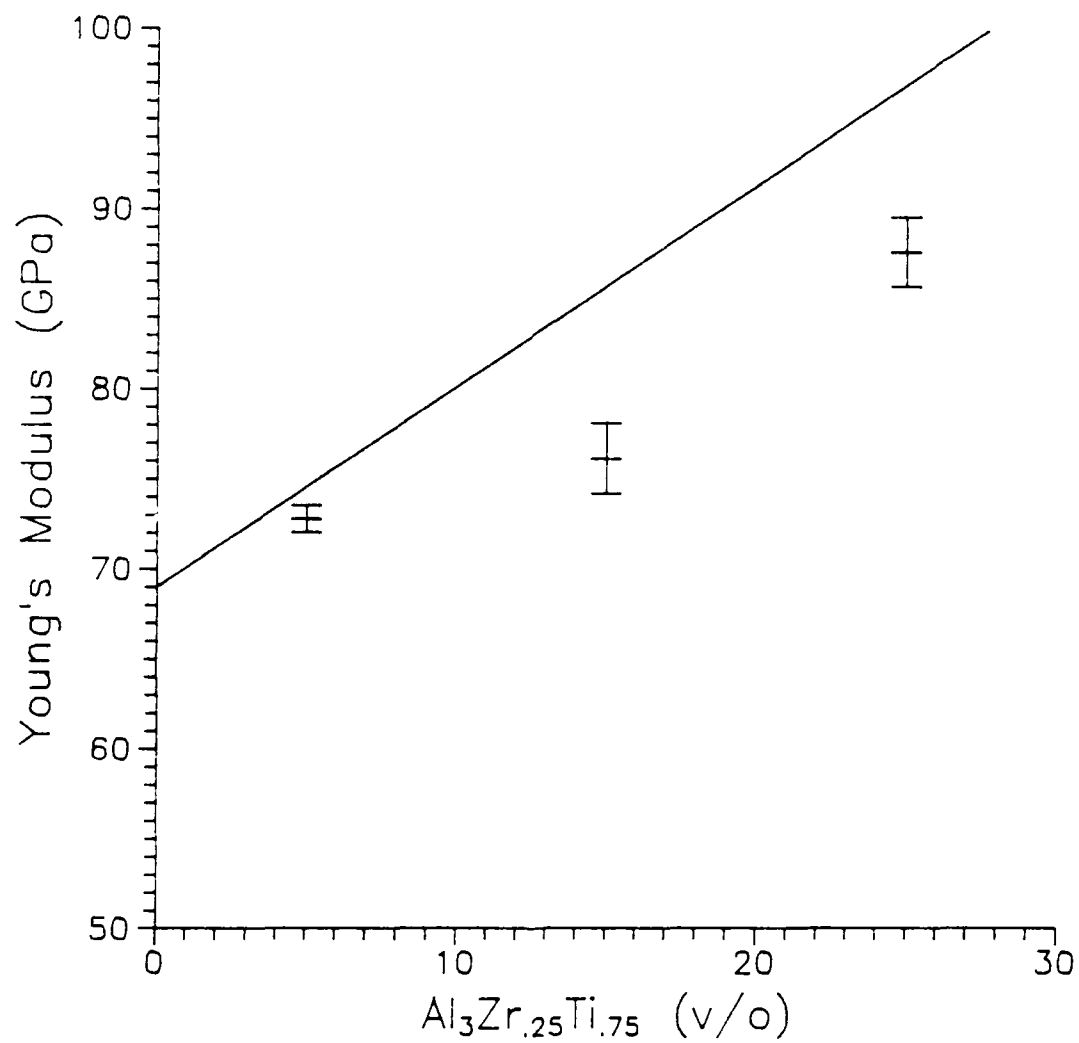
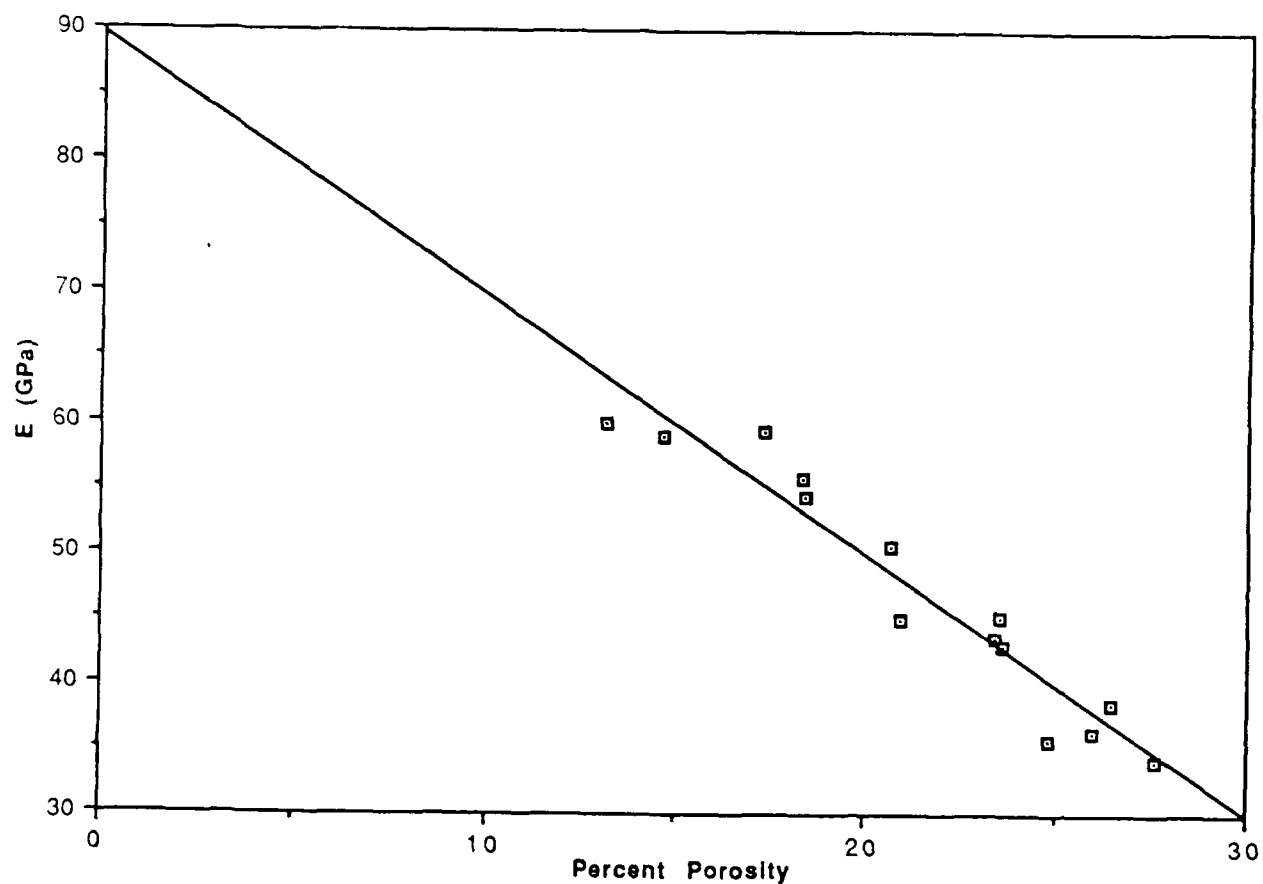


Fig. III.7. Young's Modulus vs. Percent Porosity.
Al-Al₃Zr_{0.25}Ti_{0.75} (15 v/o). As-Cast.



IV. STUDY OF INTERFACE IN Al/TiC METAL MATRIX COMPOSITES --- Rahul Mitra

The present investigation aims to study three aspects of the Al/TiC interface :

- (a) the structure of the interface,
- (b) the chemistry and thermodynamic stability of the interface and
- (c) the strength of the interface.

The first two involves the use of conventional, analytical and high resolution transmission electron microscopy while the latter involves mechanical testing.

MATERIAL

We are looking at material prepared in two different ways : as arc melted and XD™ [1]. Arc melted samples were prepared by melting Al shot mixed with TiC particles in a water cooled copper crucible in argon environment inside an arc melter at Northwestern University. The volume fraction of particles was 3.0 %. The particles were irregularly shaped and sized as 3.3 microns on an average with a distribution ranging between 1-10 microns. The Al/TiC material prepared by XD™ technique was obtained from Martin Marietta Laboratory, Baltimore, Maryland. This was obtained in the form of as extruded rods of 18 inch length and contained 15 Vol. % TiC particles. These were of two types based on particle size : 0.7 micron and 4.0 microns. The former has 0.5 volume percent large Al_3Ti particles. The modulus of elasticity for the 4.0 microns particle size material has been determined dynamically at room temperature to be 88.0 GPa.

SCANNING ELECTRON MICROSCOPY

Figs. IV.1 and IV.2 show SEM micrographs of the microstructure of as arc melted and XD™ Al/TiC respectively. The distribution is more uniform in the latter. The particles in XD™ are roughly spherical in shape and more uniform in size. The spherical shape of fully grown particles is reasonable as it provides the least possible surface area to volume ratio at any size.

TRANSMISSION ELECTRON MICROSCOPY

The interface is presently being examined by conventional microscopy techniques using an Hitachi H-700H TEM. The specimens for examination are being prepared by careful mechanical polishing up to less than 15 micron thickness followed by ion milling up to perforation. Figs. IV.3 and IV.4 show the interfaces obtained in as arc melted and XD™ Al/TiC. Both appear sharp and confirm the prediction that there would not be as much tendency for TiC to react with Al as there is for SiC to react with Al.

The XD™ material with smaller particle size has been chosen for detailed interface study as it is easier to thin the smaller particles for TEM observations. Fig. IV.5 shows a low magnification micrograph of the material. There is a distribution of particle sizes in this material. The finer particles are found inside the grain and are polygonal in shape. The larger particles are surrounded by subgrains and are present both inside and on the grain boundaries. This is illustrated in Figs. IV.6(a) and (b).

Fig. IV.7 shows a dark field micrograph from XD™ Al/TiC. Thickness fringes can be seen running parallel to the interface. A low angle boundary comprising an array of structural dislocations form the interface between the particle and the aluminium subgrain.

This can be an indication of a partially coherent interface between the matrix and the finer particles [2]. This fact needs further investigation with more of conventional and high resolution microscopy.

To study the thermodynamic stability of the interface, the arc melted Al/TiC material was heated up to 700°C, 800°C and 900°C, which are temperatures above the melting point of aluminium, in argon environment and held at that temperature for one hour. Similar treatment was attempted with Al/SiC. However, SiC particles reacted with Al giving rise to Si needles in the matrix, during arc melting only. TiC particles showed stability during arc melting and no evidence of a chemical reaction with Al. The sample held at 700°C has shown no observable interface reaction zone in TEM and SEM studies. Further analysis is being carried out to study evidence of interdiffusion between Al and TiC. The sample held at 900°C however shows formation of certain reaction products at the interface as shown in Figs. IV.8(a) and (b). Also, gaps are observed between the interface products and the matrix, showing failure of the particles to bond to Al during resolidification. This is not seen in the material held at 700°C. Fig. IV.8(c) shows a (110) zone-axis diffraction pattern from TiC. Fig. IV.8(d) is a diffraction pattern obtained by tilting the goniometer stage slightly away from the zone. We see the appearance of satellite spots. Dark field on these spots have revealed different areas of the interface. This suggests that these form partially coherent interface with the original particle [1]. One of the possibilities is the formation of Ti_3AlC by reaction between Ti_3Al and C [3,4]. Konitzer and Loretto [5] have observed the diffusion of carbon out of TiC in Ti6Al4V/TiC on heat treating the sample for 2 hours at 1000°C and quenching it. It was observed that stoichiometric TiC is surrounded by an annulus of non-stoichiometric TiC and a network

of dislocations formed to relieve the stresses due to change in carbon content. Dislocations and contrast changes from the center of the particle to the interface are observed in Figs. 8(a) and (b). The non-stoichiometric forms of titanium carbide are Ti_2C and TiC_2 [3]. Further work is being carried out, to study the composition and structure of different parts within the particle and the interfacial phases.

INTERFACIAL BOND STRENGTH ANALYSIS

An attempt has been made to study the fracture mechanism and interfacial bond strength in Al/TiC using the technique applied by Argon et.al. [6-8] to determine the interfacial bond strength in spherodized type 1045 steel, Cu-0.6% Cr alloy and maraging steel containing Fe_3C , Cu-Cr and TiC particles and Arsenault and Flom [9] for Al/SiC. Fracture in these materials takes place by nucleation and growth of voids at the interface due decohesion between matrix and particles. Voids tend to nucleate under a state of triaxial or hydrostatic stress and interfacial tensile stress at the interface between particle and matrix. According to theoretical analysis of Argon et.al. [7], the interfacial tensile stress can be expressed as :

$$\sigma_{\pi} = \sigma_{\tau} + Y(e^p)$$

where σ_{τ} is the local triaxial tensile stress and $Y(e^p)$ is the true tensile flow stress corresponding to local average plastic strain in absence of the particle. This analysis assumes that (1) the second phase particles are of equiaxed shape, (2) the volume fraction of the second phase is small and (3) the particles are undeformed. The triaxial stress along the radial line in the plane of the notch in the tensile specimen is obtained from Neuber analysis and is expressed as :

$$\sigma_T/\sigma_o = c/\{1-(r/a')^2\}^{1/2} \quad (z = 0)$$

where σ_T/σ_o represents the triaxiality, σ_T is the negative pressure, σ_o is the flow stress or average ligament stress, z is the vertical distance along the tensile axis of the sample and r is the distance from the tensile axis. The triaxiality reaches its maximum at the notch, that is, at $r=a$, where $2a$ is the ligament diameter. Hence, $r=a$ is taken for calculation. c and a' are expressed as :

$$c = \{1 + a/R + (1 + a/R)^{1/2}\}/2\{2 + a/R + (1 + a/R)^{1/2}\}$$

$a' = a(1 + a/R)/(a/R)$, where R is the notch radius.

Notched tensile samples were made from as-arc melted Al/TiC and pulled in tension until fracture and one set of the fractured halves was studied using SEM. SEM fractographs are shown in Figs. IV.9 (a) and (b). A bimodal distribution of voids can be seen. The smaller ones form in the soft aluminium matrix during ductile fracture and the larger ones form around the particles or clusters. Particles can be seen sitting inside the dimples. Some of them appear to have cracked in tension as shown in Fig. IV.9 (b).

The other set of fractured halves was vertically sectioned, mounted in resin and polished for metallographic examination. Figs. IV.10 (a) and (b) show crack profiles from near the notch. Voids are observed in the matrix, where there is a localised increase in concentration of second phase. This happens due to high stress concentrations occurring in such regions during tension. Critical plastic strain for void nucleation is reached earlier in regions of higher particle concentration. Voids are not seen to nucleate as we move down the z -axis. Figs. IV.11 (a) and (b) show crack profiles from the remaining fracture surface. From our observations, we conclude that fracture takes place by cracking of particles and formation and growth of voids around them and in the matrix. Particles do

not appear to have decohered from the matrix. Thus, we can estimate only the lower bound limit of interfacial bond strength. The true stress corresponding to true plastic strain at fracture has been determined to be 178 MPa. This gives the interfacial bond strength as 460.0 MPa, which is more than the ultimate tensile strength of the matrix, pure aluminium. Practically, it can be inferred, the interfacial bond strength is much higher than 460.0 MPa as the crack propagates mainly through the matrix. Thus, this technique can only be used for a rough comparison of bond strengths between different dispersoids and the same matrix. Further experiments with even lower volume fraction of TiC particles (1.0 %) is being planned to verify the above result. Also, some other dispersoid as TiB_2 will be used to compare the results.

An analysis involving deforming the sample and annealing it to form voids of equilibrium size and shape so as to measure the contact angle is in progress. This technique has been previously applied by Easterling et.al. [8]. The estimation of contact angle will help in determining the work of adhesion between the particle and the matrix.

REFERENCES

1. A.R.C. Westwood, Metall. Trans., Vol. 19A, p. 749 (1988)
2. P. Hirsch, A. Howie, R. Nicholson, D.W. Pashley and M.J. Whelan, Electron Microscopy of Thin Crystals, Robert E. Krieger Publishing Company, Malabar, Florida, Chapter 14, p. 317 (1977)
3. P. Villars and L.D. Calvert, Pearson's handbook of crystallographic data for intermetallic phases, American Society of Metals, Metals Park, Oh 44073, Vol. 1, p. 710; Vol. 2, p. 1583 (1985)

4. M.E. Fine and J.G. Conley, Metall.Trans. Vol. 21A, p. 2609 (1990)
5. D.J. Konitzer and M.H. Loretto, Acta Metall., Vol. 37, p. 397 (1989)
6. A.S. Argon, J. Im and A. Needleman, Metall. Trans., Vol. 6A, p. 815 (1975)
7. A.S. Argon, J. Im, R. Safoglu, Metall. Trans., Vol. 6A, p. 825 (1975)
8. A.S. Argon and J. Im, Metall. Trans., Vol. 6A, p. 839 (1975)
9. Y. Flom and R.J. Arsenault, Mater. Sci. and Eng., Vol. 77, p.191 (1986)
10. K.E. Easterling, H. Fischmeister and E. Navara, Powder Metall., Vol. 16, p.128 (1973)



Fig. IV.1. SEM micrograph of as arc melted Al/TiC.

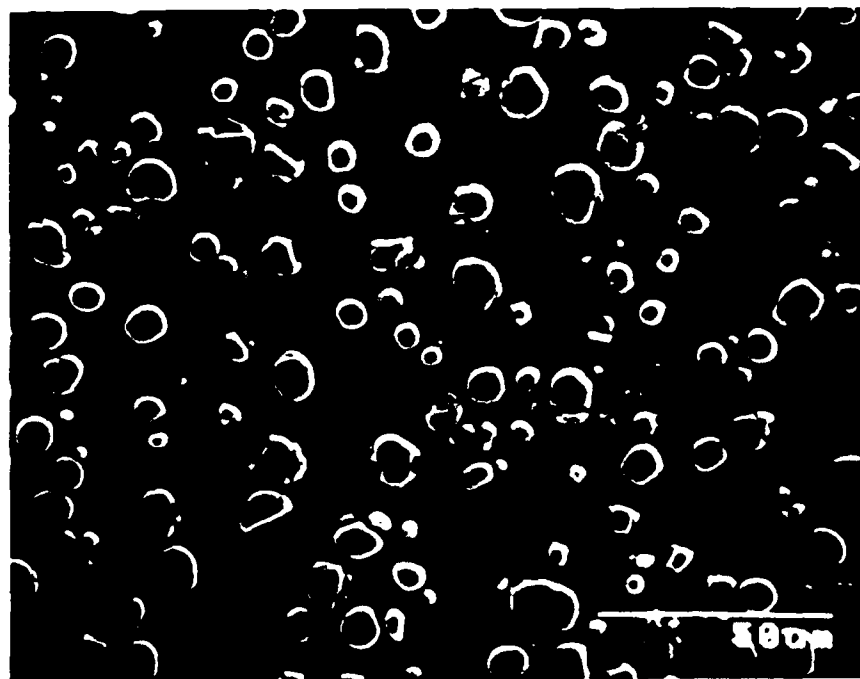


Fig. IV.2. SEM Micrograph of XD™ Al/TiC.

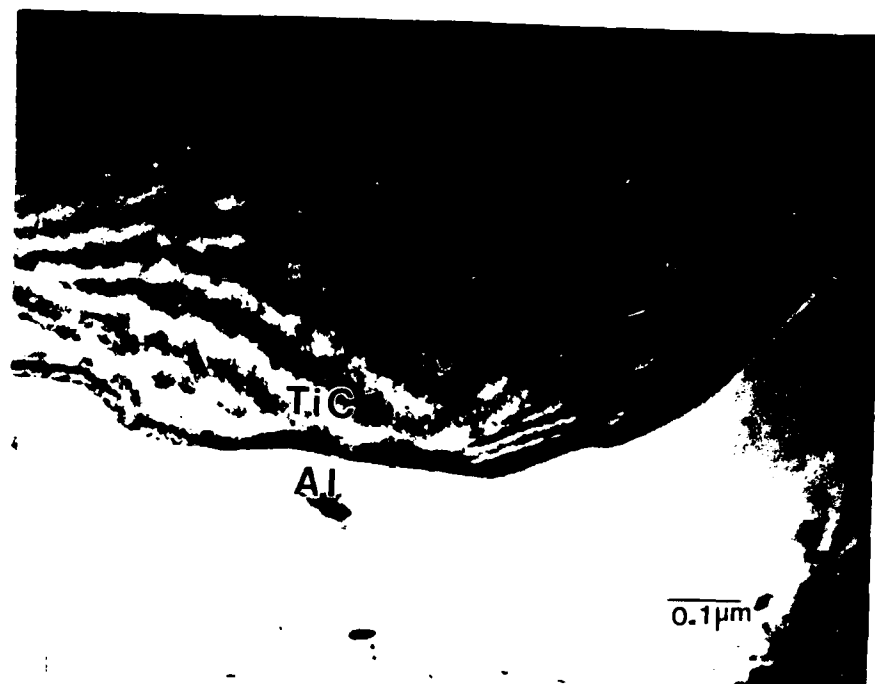


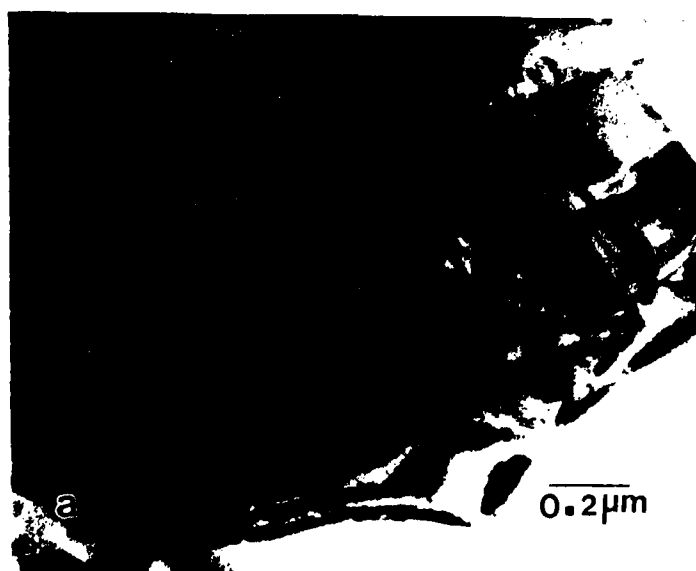
Fig. IV.3. TEM micrograph of Al/TiC interface obtained in arc melting.



Fig. IV.4. TEM micrograph of Al/TiC interface obtained in XD™ Al/TiC.



Fig. IV.5. Low magnification TEM micrograph of XD™ Al/TiC. This shows a large blocky Al_3Ti particle.



Figs. IV.6(a) and (b). TEM micrographs showing distribution of particles within and at boundaries of grain.

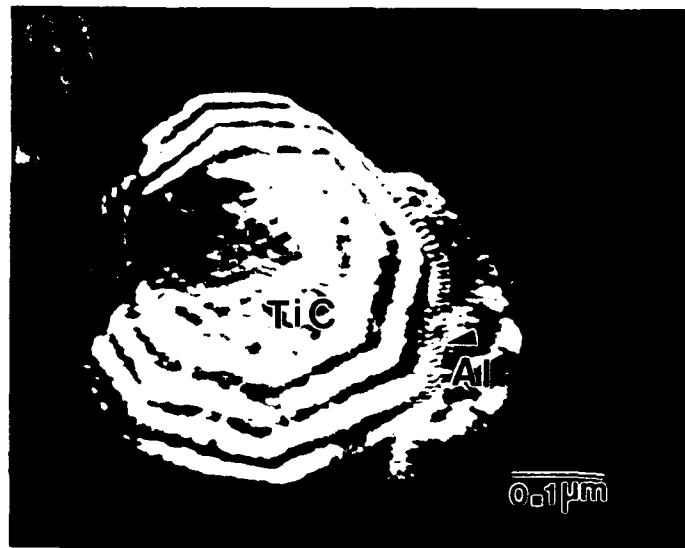
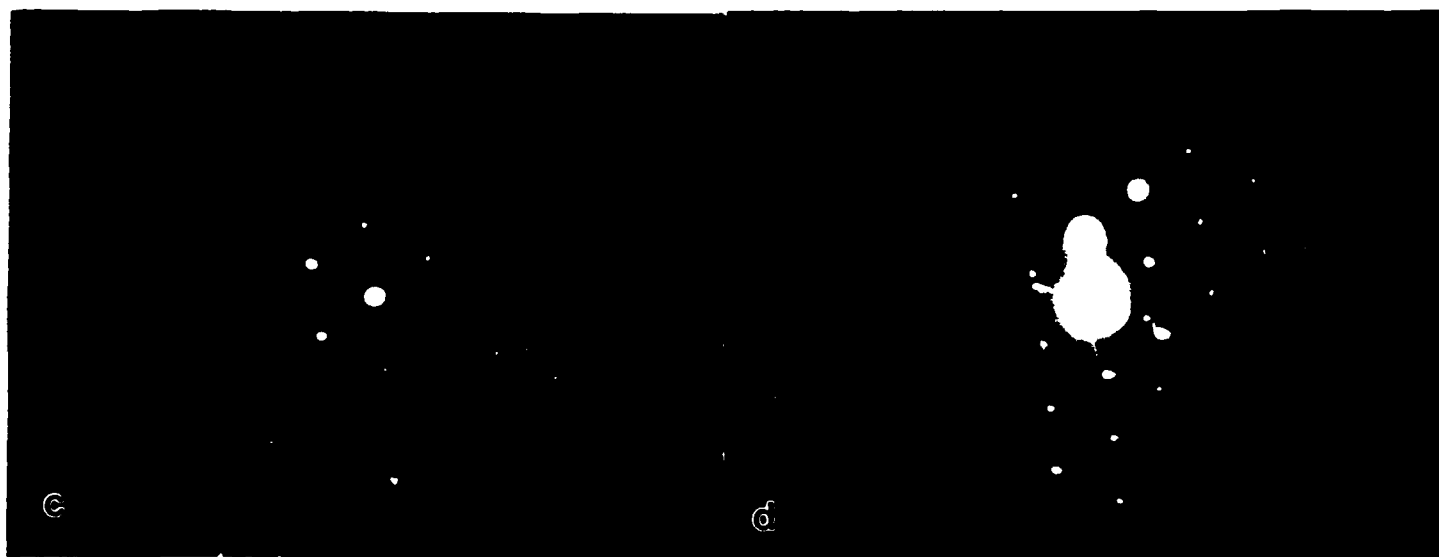
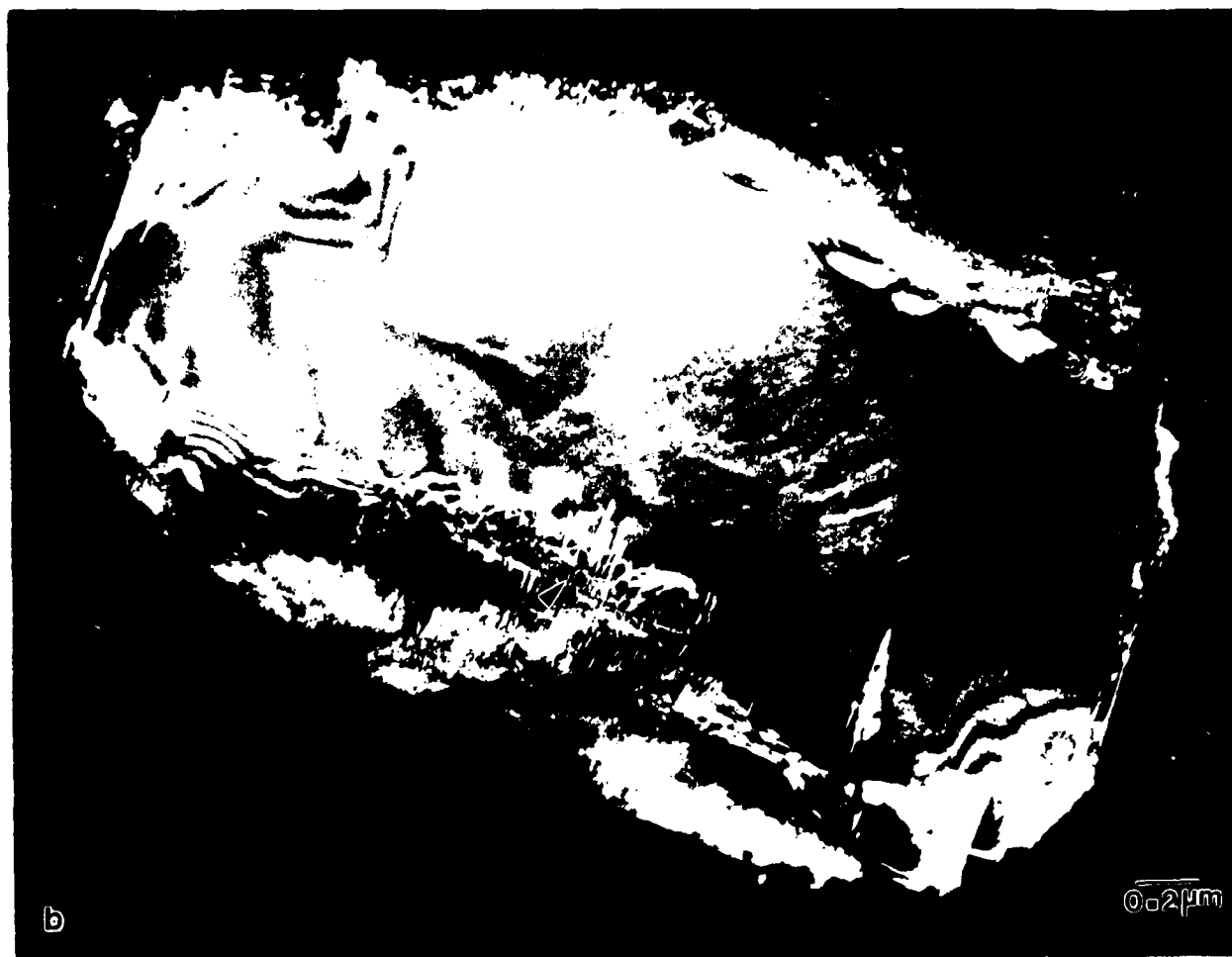


Fig. IV.7. Dark field TEM micrograph showing a low angle boundary forming the interface between TiC particle and Al subgrain.



Fig. IV.8. TEM analysis of Al/TiC after holding it at 900°C for one hour. (a). Bright field micrograph showing interface reaction products and variable contrast within the particle.



(b) Dark field micrograph taken from (002) spot. Needle like features can be seen at the interface. (c) Near zone axis (110) diffraction pattern. (d) Diffraction pattern showing spots from the reaction products on tilting slightly off from the (110) zone-axis.

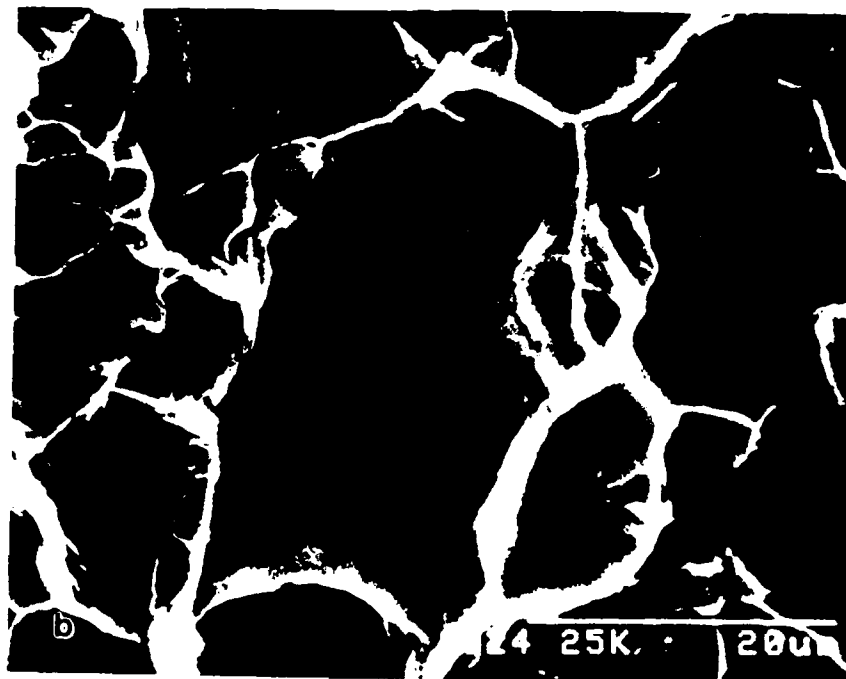
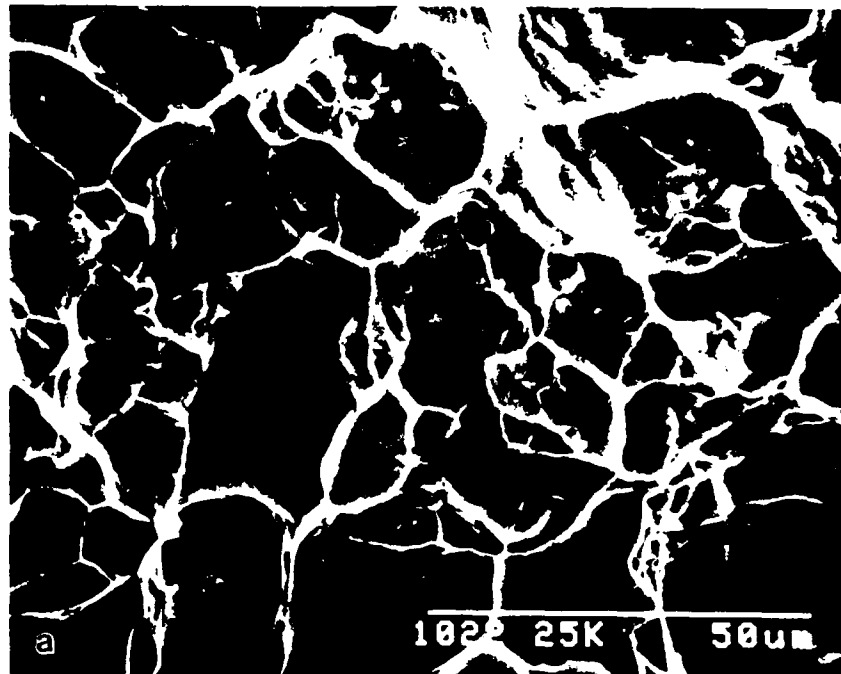
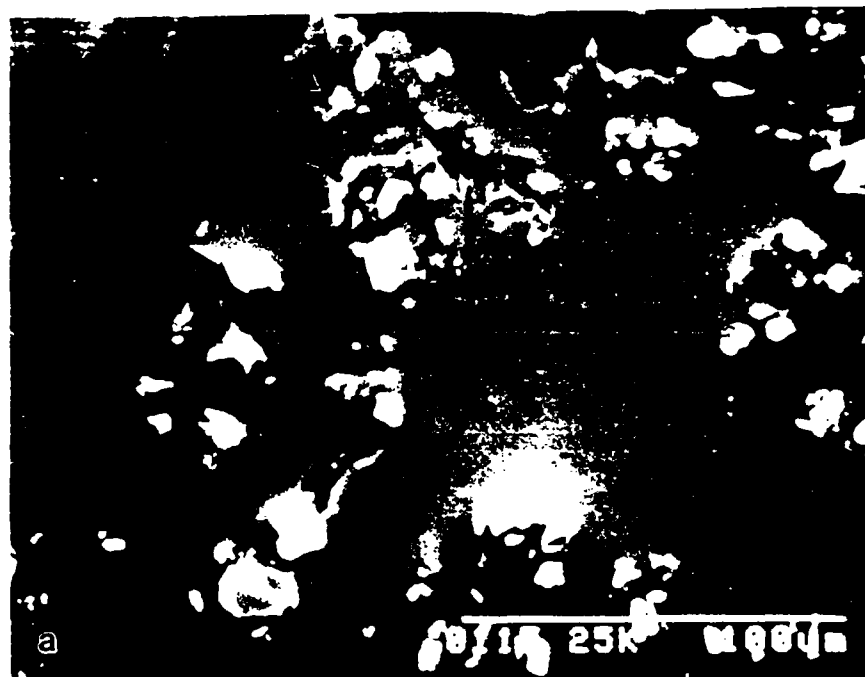


Fig. IV.9. (a) Low magnification SEM fractograph as arc melted Al/TiC. Bimodal distribution of voids can be seen with smaller ones in the matrix and the larger ones forming around the cracked particles. (b) A high magnification micrograph of a void with a cracked particle inside.



Figs. IV.10(a) and (b). Crack profiles near the notch. Voids can be observed in the matrix, especially, in regions of higher local concentrations of TiC particles.

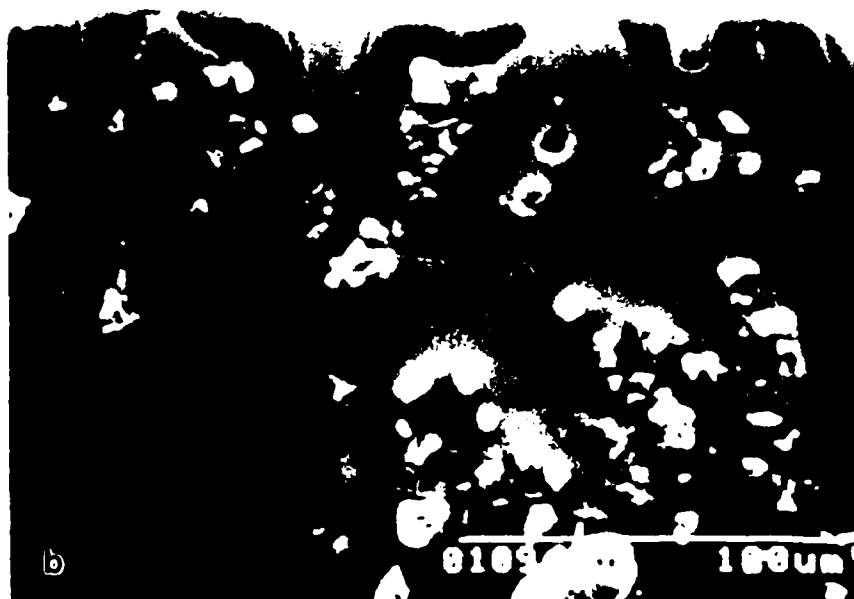
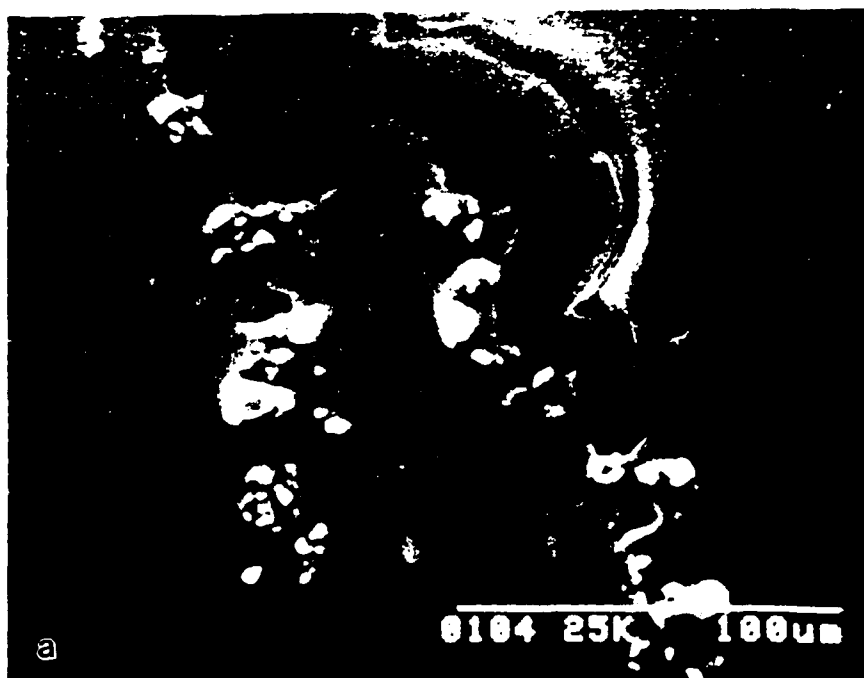


Fig. IV.11(a) and (b). Crack profiles from rest of the fracture surface.

JOHN J. BLUM

OBJECTIVE A challenging applied research position in the materials science and engineering field utilizing skills in alloy development, materials selection and product design.

EDUCATION **NORTHWESTERN UNIVERSITY**, Evanston, IL
Ph.D., Materials Science and Engineering (expected Aug. '91)
RESEARCH ADVISORS: Professor Morris E. Fine and Professor Julia R. Weertman

UNIVERSITY OF ILLINOIS at CHICAGO, Chicago, IL
B.S., Metallurgy (June '87)

EXPERIENCE **NORTHWESTERN UNIVERSITY**, Evanston, IL (Sept. '87 - present)
Research Assistant: Investigated and compared physical properties of a mechanically alloyed aluminum matrix with a dispersion of stable oxides (spinel or alumina) as a function of oxide volume fraction, temperature and strain rate. Determined optimum periods for mechanical alloying. Characterized the microstructures: grain size, grain aspect ratios, particle size, particle distribution and volume fraction via TEM analysis. Designed an extrusion apparatus for aluminum alloys. Skilled in the use of servo-hydraulic testing machines, creep testing equipment, mechanical measurements at elevated temperatures, acoustic property evaluation, thermal expansion equipment, transmission electron, scanning electron and optical microscopy and various metallographic techniques.

AMOCO RESEARCH CENTER, Naperville, IL (Feb. '86 - Sept. '87)
Part-time Metallurgical Technician: Sectioned, mounted, polished, etched and photographed failed petro-chemical equipment for metallographic evaluation and failure analysis. Polished carbon-fiber polymer composites for evaluation of processing parameters. Standardized materials specifications for high temperature use. Investigated and surveyed relevant material pertaining to the failure of materials used in the fabrication of flare tips. Versed in failure analysis, metallography and the petro-chemical industry.

UNIVERSITY OF ILLINOIS at CHICAGO, Chicago, IL (March '85 - Feb. '86)
Research Aide, Welding Laboratory: Evaluated microstructures of welding zones and weld parameters. Assembled and calibrated a creep testing apparatus.

UNIVERSITY OF ILLINOIS at CHICAGO, Chicago, IL (Sept. '85 - Dec. '85)
Teaching Assistant, Physical Metallurgy I Laboratory: Instructed undergraduate students in the use of laboratory equipment. Conducted and supervised laboratory experiments.

PUBLICATIONS J.J. Blum, M.E. Fine and J.R. Weertman, "Mechanical Properties of Al-Spinel and Al-Alumina Composites", to appear in Scripta Materialia.

PRESENTATIONS Mechanical Properties of Al-Spinel and Al-Alumina Composites, Amoco/University Poster Session, Amoco Research Center, Naperville, IL (Oct. '90)
"Mechanical Properties of Al-Spinel and Al-Alumina Composites as a Function of Time and Temperature", to be presented at AIME Annual Meeting, New Orleans, La. Coauthors: M.E. Fine and J.R. Weertman. (Feb. '91)

AWARDS/HONORS American Society for Metals Student Scholar Award. (1986)
Industrial Scholar Award, Department of Civil Engineering, Mechanics and Metallurgy, University of Illinois at Chicago. (1985)
President Materials Engineering Club, University of Illinois at Chicago. (1986)
Illinois State Scholar. (1983)

AFFILIATIONS Member of American Society for Metals and The Metallurgical Society of AIME.

NEIL R. BROWN

Education

Northwestern University, Fall 1988-present. PhD candidate in MS&E.

Rice University, Houston, TX

BS, Materials Science, May 1988 GPA: 3.03

Del Norte High School, Albuquerque, NM GPA: 3.90

Honors

National Merit Scholar

Rice University President's Honor Role

Rice University Board of Governors' Scholarship Recipient

Second Place in the State of New Mexico Debate Tournament, 1984

Delegate to New Mexico Boys' State

Activities

Rice:

Hanszen College Cabinet Section Representative	1985-1987
Hanszen College Acquisitions & Improvements Committee	1986-1988
Freshman Advisor	1986-1987
Waterpolo Club Team	1984-1987
Soccer Club Team	1984-1988

High School:

Debate, Speech, Chess Teams	1980-1984
Staters Club Vice President	1983-1984

Work and Research Experience

Materials Consultant for PDA Engineering 3754 Hawkins, Albuquerque, NM Assistant Director of Small Business Innovative Research Grant for the U.S. Navy to produce graphite fibers with thin uniform phenolic resin coatings.	Summer 1988
Materials Consultant for PDA Engineering Materials testing, processing, and treatment and the design and construction of a prototype continuous plasma unit for the treatment of composite fibers.	Summer 1987
Senior Research Project in High Temperature Superconductors Research Assistant under Dr. J. M. Roberts, professor of Materials Science. Studying interface properties as a function of Ag, Au content.	1987-1988

PHILIP A. EARVOLINO

Education:

Northwestern University, Evanston, IL, July 1988-present. PhD candidate in Materials Science and Engineering.

University of Pennsylvania, Philadelphia, PA, September 1984-May 1988. B.S.E. in Bioengineering. Magna cum laude. GPA: 3.8/4.0

Holliston High School, Holliston, MA, September 1980-June 1984. Class Valedictorian.

Work Experience:

September 1987-December 1987. Biomaterials research, U. of Penn. Lead to senior thesis on development of an oxygen microelectrode for monitoring in vivo response of a biologically active glass.

September 1986-May 1987. Hospital of the University of Pennsylvania, Philadelphia, PA. Researcher in human genetics laboratory.

Awards, Honors:

Recipient of D.O.D. fellowship for current research.

Schwann Bioengineering Award, University of Pennsylvania. Awarded to best student in bioengineering department.

RESUME

NAME: RAHUL MITRA

[REDACTED]

EDUCATION:

1988- Graduate Research Assistant, Northwestern University

1984-1988 Indian Institute of Technology, Kharagpur, India. Graduated with B.Tech (Hons.) degree in Metallurgical Engineering May, 1988. CGPA = 9.11 out of 10.0.

AWARDS: National Talent Scholarship and the Certificate of Merit, National Council of Educational Research and Training, New Delhi, 1982-1988.

Institute Silver Medal for the academic year 1987-88 for best among the graduating students in Metallurgical Engineering.

General Proficiency Prize for standing First in order of merit among the Final year students of B.Tech (Hons.) course in Metallurgical Engineering for academic year 1987-88.

Bengal Ingot Award (Silver Medal) for the year 1988 for the best project work in Foundry at undergraduate level from the Institute of Indian Foundrymen.

"Indranil Award for Metallurgy" for the year 1987-88 for securing First position in Metallurgical Engineering of Indian Institute of Technology, Kharagpur from the Mining, Geological and Metallurgical Institute of India.

First prize in All India Essay Contest '87 organized by Metallurgical Engineering Society, V.R.C.E., Nagpur, during the year 1986-87. The topic was "Processing of Complex Cu-Pb-Zn ores for Extraction of Metallic Values".